

Spin liquid versus long range magnetic order in the frustrated body-centered tetragonal lattice

Sébastien Burdin

*Univ. Bordeaux, LOMA, UMR 5798, F-33400 Talence, France and
CNRS, LOMA, UMR 5798, F-33400 Talence, France*

Christopher Thomas

*Institut de Physique Théorique, CEA-Saclay, 91191 Gif-sur-Yvette, France
International Institute of Physics, Universidade Federal do Rio Grande do Norte, 59078-400 Natal-RN, Brazil and
Instituto de Física, UFRGS, 91501-970 Porto Alegre-RS, Brazil*

Catherine Pépin

Institut de Physique Théorique, CEA-Saclay, 91191 Gif-sur-Yvette, France

Alvaro Ferraz

*International Institute of Physics, Universidade Federal do Rio Grande do Norte, 59078-400 Natal-RN, Brazil and
Departamento de Física Teórica e Experimental, Universidade Federal do Rio Grande do Norte, 59072-970 Natal-RN, Brazil*

Claudine Lacroix

*Institut Néel, Université Grenoble-Alpes, F-38042 Grenoble, France and
Institut Néel, CNRS, F-38042 Grenoble, France*

(Dated: May 9, 2021)

The quantum Heisenberg model is studied in the geometrically frustrated body-centered tetragonal lattice (BCT lattice) with antiferromagnetic interlayer coupling J_1 and intralayer first and second neighbor coupling J_2 and J_3 . Using a fermionic representation of the spin $1/2$ operators, we introduce a variational method: each interaction term can be decoupled partially in the purely magnetic Weiss and in the spin-liquid (SL) mean-field channels. We find that the most stable variational solutions correspond to the three different possible long range magnetic orders that are respectively governed by J_1 , J_2 , and J_3 . We show that magnetic and SL parameters do not coexist, and we characterize three different purely SL non-magnetic solutions that are variationally the second most stable states after the purely magnetic ones. The degeneracy lines separating the purely magnetic phases do not coincide with the ones separating the purely SL phases. This suggests that quantum fluctuations induced by the frustration between J_1 - J_2 - J_3 coupling should destroy magnetic orders and stabilize the formation of SL in large areas of parameters. The SL solution governed by J_1 breaks the lattice translation symmetry. This Modulated SL is associated to a commensurate ordering wave vector $(1,1,1)$. Remarking that four different fits of experimental data on URu_2Si_2 locate this material with BCT lattice very close to the degeneracy line between J_1 and J_3 but well inside the Modulated SL, we suggest that frustration might be a key ingredient for the formation of the Hidden order phase observed in this compound. Our results also underline possible analogies between different families of correlated systems with BCT lattice, including unconventional superconductors. Also, the general variational method introduced here can be applied to any other system where interaction terms can be decoupled in two different mean-field channels.

I. INTRODUCTION

The body-centered tetragonal (BCT) lattice is one of the 14 three-dimensional lattice types.¹ This standard crystalline structure is realized in several strongly correlated electron materials with unusual magnetic and transport properties. Among the heavy fermion systems,^{2,3} different examples of materials with rare earth atoms on a BCT lattice have been intensively studied for the last decades: in URu_2Si_2 , a still mysterious Hidden order (HO) phase was discovered in 1986, that appears below the critical temperature $T_{HO} \approx 17$ K close to a pressure-induced antiferromagnetic (AF) transition;^{4,5} in YbRh_2Si_2 and CeRu_2Si_2 , non-Fermi liquid properties are observed in the vicinity of AF quantum phase transitions, that are still poorly understood;⁶⁻⁹ CeCu_2Si_2 was the first (heavy fermion) material where unconventional superconductivity was discovered in 1979 close to an AF transition;¹⁰ CePd_2Si_2 also exhibits unconventional superconduc-

tivity related to an AF transition.^{11,12} Today, each one of these compounds can yet be considered as one entire field of research. It is noticeable that the link between AF ordering and unconventional superconductivity has also been suggested in other families of correlated materials with BCT symmetry: the cuprate superconductors, discovered in 1986 by Bednorz and Muller,¹³ whose AF insulating parent compounds include La_2CuO_4 and $\text{Sr}_2\text{CuO}_2\text{Cl}_2$. In these cases, the AF order originates from the Cu atoms that form a BCT crystal. But the relevant physics there is mainly two-dimensional, the BCT structure being only involved in the formation of square-lattice layers of Cu atoms that order antiferromagnetically.

The BCT lattice can also be considered as a prototype three-dimensional frustrated system. Important theoretical developments were made in the past years about the unconventional magnetic properties of the BCT lattice using a classical Heisenberg model. These works were motivated by the rich magnetic phase diagram of iron based materials like FePd pos-

sibly doped with Rh, with a main focus on the competition between ferromagnetic, AF, and helical orders.¹⁴⁻¹⁹ Tuning the interaction parameters made possible the description of different phases in the XY and Heisenberg models with thermal and quantum fluctuations. It was also shown that magnetic fluctuations as magnons excitations can help in the stability of long-range order.

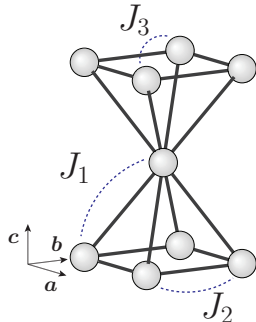


FIG. 1. BCC lattice and the J_1 , J_2 , and J_3 interactions. Lattice constants are a in the \mathbf{a} , \mathbf{b} directions and c along c .

In this paper, we analyze the ground states of a frustrated J_1 - J_2 - J_3 quantum Heisenberg model on a BCC lattice as illustrated by figure 1. We are aware that a complete exact determination of its expected-to-be rich phase diagram would not be realistic and we thus need to do some approximations. Here, we introduce and use a variational mean-field method that allows to decouple the Heisenberg interaction terms partially in the standard Weiss and in the modulated spin liquid (MSL) channels. Since the MSL state has been initially introduced as a scenario for the HO state in URu_2Si_2 ,²⁰⁻²² applications to this compound are considered as one motivation. However, the method which is developed here could be adapted to other correlated systems with BCC structure.

The paper is organized as follows: section II introduces the concept of MSL, the model, the mean-field decoupling, and the variational method. General results including phase diagrams are analyzed for $J_3 = 0$ and all T in section III, and for $T = 0$ and all J_3 in section IV. We will see how geometric frustration that is intrinsic to the model may help stabilizing a MSL ordered ground state. Applications to real correlated materials with BCC lattice are discussed in section V.

II. MODEL AND METHOD

A. The concept of modulated spin liquid (MSL)

The expression spin liquid was originally introduced in 1976 by contrast with spin glasses, in order to describe the dynamical properties of a disordered spin system.²³ Nonetheless the concept of spin liquid within quantum Heisenberg models on frustrated geometries usually also refers to the Resonant Valence Bond (RVB) state proposed by Fazekas and Anderson in 1974 on the triangular lattice.²⁴ Later, Baskaran, Zou, and Anderson have proposed that RVB spin-liquid correla-

tions could act like a magnetic glue for the Cooper pair formation in cuprate superconductors.²⁵⁻²⁸ Within this scenario, the AF Néel ordered state formed by the Cu square lattice layers in the insulating parent compounds is destabilized by charge fluctuations induced by doping on the O sites. The MSL scenario proposed for URu_2Si_2 was inspired by the spin-liquid scenario for cuprates. Even if the underlying BCC lattice is shared by these two families of systems, the microscopic physics in URu_2Si_2 is of course quite different and the long range orders invoke correlations in three-dimensions. Whether a system can have a true spin-liquid ground state or not has been a long standing issue, but some good evidences of possible spin-liquid ground states have been proposed for the Heisenberg model on frustrated lattices.²⁹⁻³² It has also been observed from numerical calculations that spin-liquid disordered states can be very close in energy to dimer ordered states.^{33,34} In general, spin dimer orders refer to bond orders that are characterized by a given periodic pattern of disconnected dimers. The proposed MSL state can be thought of as a kind of spin dimer commensurate ordered state where two different dimers may be connected to a same site. Such a dimer ordered state may also be named valence bond crystal³² especially when it is characterized by bosonic triplet excitations. Here, we prefer use the name MSL because its magnetic excitations are deconfined Abrikosov fermions.

In previous works, the competition between AF and MSL orders on a square lattice²⁰ and on a BCC lattice²¹ was tuned phenomenologically by introducing two independent nearest neighbor coupling J_{AF} and J_{SL} . Here, we study this competition as an intrinsic effect associated to the geometric frustration in the J_1 - J_2 - J_3 quantum Heisenberg model on the BCC lattice. We then introduce a variational method that allows to treat the system in a mean field approximation, where the interaction on each lattice bond can be decoupled in two channels, the magnetic and the spin liquid. The relative weight of each decoupling channel is determined by minimizing the free energy of the system.

B. Model and method of calculation

1. The J_1 - J_2 - J_3 model

The J_1 - J_2 - J_3 model is defined by the following quantum Heisenberg Hamiltonian:

$$H = \sum_{\langle \mathbf{R}, \mathbf{R}' \rangle} \sum_{\sigma \sigma'} J_{\mathbf{R}\mathbf{R}'} \chi_{\mathbf{R}\sigma}^\dagger \chi_{\mathbf{R}\sigma'} \chi_{\mathbf{R}'\sigma'}^\dagger \chi_{\mathbf{R}'\sigma}, \quad (1)$$

where $\chi_{\mathbf{R}\sigma}^\dagger$ ($\chi_{\mathbf{R}\sigma}$) is the creation (annihilation) fermionic operator that represents quantum spins 1/2, and satisfy the local constraints $\sum_{\sigma=\uparrow, \downarrow} \chi_{\mathbf{R}\sigma}^\dagger \chi_{\mathbf{R}\sigma} = 1$. The antiferromagnetic interactions $J_{\mathbf{R}\mathbf{R}'}$ connects two sites \mathbf{R} and \mathbf{R}' on a BCC lattice, and can take three possible values J_1 , J_2 , $J_3 > 0$, as indicated on figure 1.

2. Variational method

In a very oversimplified classical mean field approach and considering the specific connectivity of the BCT lattice, we expect that competition between different Weiss mean fields may reveal degenerate frustrated ground states. Hereafter, we go beyond this classical picture, and we introduce quantum correlation effects at a mean field level within a spin-liquid RVB-like decoupling on each bond. First we formally split the interaction term on each bond into two different contributions:

$$J_i \equiv J_i^{\text{Weiss}} + J_i^{\text{SL}} \equiv J_i \cos^2(\alpha_i) + J_i \sin^2(\alpha_i), \quad (2)$$

where α_1 , α_2 , and α_3 are variational parameters. Hereafter, each interaction term will be treated within a mixed mean-field approximation on each bond: the mean-field decoupling will be made partially in the Weiss channel, and partially in the SL channel. The extreme cases $\alpha_i = 0$ and $\alpha_i = \pi/2$ correspond to a decoupling in the purely classical Weiss channel and in the purely SL channel, respectively. In the following, the three decoupling variational parameters $\alpha_i \in [0, \pi/2]$ will be determined self-consistently as functions of J_1 , J_2 and J_3 in order to minimize the free energy of the system.

3. General mean-field decoupling

Generalizing the procedure developed in Refs. 20 and 21, and invoking the variational splitting Eq. 2, the Heisenberg Hamiltonian (eq. (1)) is decoupled for each bond $\mathbf{R}\mathbf{R}'$ using appropriated Hubbard-Stratonovich transformations as follows:

$$\begin{aligned} & J_i^{\text{Weiss}} \sum_{\sigma\sigma'} \chi_{\mathbf{R}\sigma}^\dagger \chi_{\mathbf{R}\sigma'} \chi_{\mathbf{R}'\sigma'}^\dagger \chi_{\mathbf{R}'\sigma} \\ & \approx J_i^{\text{Weiss}} \sum_{\sigma} \left(\sigma m_{\mathbf{R}} \chi_{\mathbf{R}'\sigma}^\dagger \chi_{\mathbf{R}'\sigma} + \sigma m_{\mathbf{R}'} \chi_{\mathbf{R}\sigma}^\dagger \chi_{\mathbf{R}\sigma} \right) \\ & - 2J_i^{\text{Weiss}} m_{\mathbf{R}} m_{\mathbf{R}'}, \end{aligned} \quad (3)$$

where $m_{\mathbf{R}}$ is the local contribution from site \mathbf{R} to the magnetic Weiss field, with $\sigma = \uparrow, \downarrow \equiv +, -$, and :

$$\begin{aligned} & J_i^{\text{SL}} \sum_{\sigma\sigma'} \chi_{\mathbf{R}\sigma}^\dagger \chi_{\mathbf{R}\sigma'} \chi_{\mathbf{R}'\sigma'}^\dagger \chi_{\mathbf{R}'\sigma} \\ & \approx J_i^{\text{SL}} \sum_{\sigma} \left(\varphi_{\mathbf{R}\mathbf{R}'}^* \chi_{\mathbf{R}\sigma}^\dagger \chi_{\mathbf{R}'\sigma} + c.c. \right) + J_i^{\text{SL}} |\varphi_{\mathbf{R}\mathbf{R}'}|^2, \end{aligned} \quad (4)$$

where $\varphi_{\mathbf{R}\mathbf{R}'}^* \equiv \varphi_{\mathbf{R}'\mathbf{R}}$ denotes the spin-liquid field on the bond $\mathbf{R}\mathbf{R}'$. Hereafter, the Hubbard-Stratonovich fields are replaced by their mean-field values, which are given by free energy saddle point conditions:

$$m_{\mathbf{R}} = \frac{1}{2} \sum_{\sigma} \sigma \langle \chi_{\mathbf{R}\sigma}^\dagger \chi_{\mathbf{R}\sigma} \rangle, \quad (5)$$

$$\varphi_{\mathbf{R}\mathbf{R}'} = - \sum_{\sigma} \langle \chi_{\mathbf{R}\sigma}^\dagger \chi_{\mathbf{R}'\sigma} \rangle. \quad (6)$$

The self-consistency of the mean-fields is established from the following mean-field Lagrangian:

$$\mathcal{L} = \mathcal{L}_1 + \mathcal{L}_2 + \mathcal{L}_3 + \sum_{\mathbf{R}\sigma} \chi_{\mathbf{R}\sigma}^\dagger (\partial_\tau + \lambda_{\mathbf{R}}) \chi_{\mathbf{R}\sigma} - \sum_{\mathbf{R}} \lambda_{\mathbf{R}}, \quad (7)$$

with

$$\begin{aligned} \mathcal{L}_1 \equiv & \sum_n \sum_{\langle \mathbf{R} \in P_n, \mathbf{R}' \in P_{n+1} \rangle} \left[J_1^{\text{SL}} \sum_{\sigma} \left(\varphi_{\mathbf{R}\mathbf{R}'}^* \chi_{\mathbf{R}\sigma}^\dagger \chi_{\mathbf{R}'\sigma} + c.c. \right) \right. \\ & + J_1^{\text{Weiss}} \sum_{\sigma} \left(\sigma m_{\mathbf{R}} \chi_{\mathbf{R}'\sigma}^\dagger \chi_{\mathbf{R}'\sigma} + \sigma m_{\mathbf{R}'} \chi_{\mathbf{R}\sigma}^\dagger \chi_{\mathbf{R}\sigma} \right) \\ & \left. + J_1^{\text{SL}} |\varphi_{\mathbf{R}\mathbf{R}'}|^2 - 2J_1^{\text{Weiss}} m_{\mathbf{R}} m_{\mathbf{R}'} \right], \end{aligned} \quad (8)$$

where P_n denotes sites of the planar layer n oriented in the a, b crystallographic directions indicated on figure 1, and:

$$\begin{aligned} \mathcal{L}_2 \equiv & \sum_{n\sigma} \sum_{\langle \mathbf{R}, \mathbf{R}' \rangle \in P_n} \left[J_2^{\text{SL}} \sum_{\sigma} \left(\varphi_{\mathbf{R}\mathbf{R}'}^* \chi_{\mathbf{R}\sigma}^\dagger \chi_{\mathbf{R}'\sigma} + c.c. \right) \right. \\ & + J_2^{\text{Weiss}} \sum_{\sigma} \left(\sigma m_{\mathbf{R}} \chi_{\mathbf{R}'\sigma}^\dagger \chi_{\mathbf{R}'\sigma} + \sigma m_{\mathbf{R}'} \chi_{\mathbf{R}\sigma}^\dagger \chi_{\mathbf{R}\sigma} \right) \\ & \left. + J_2^{\text{SL}} |\varphi_{\mathbf{R}\mathbf{R}'}|^2 - 2J_2^{\text{Weiss}} m_{\mathbf{R}} m_{\mathbf{R}'} \right], \end{aligned}$$

$$\begin{aligned} \mathcal{L}_3 \equiv & \sum_{n\sigma} \sum_{\langle\langle \mathbf{R}, \mathbf{R}' \rangle\rangle \in P_n} \left[J_3^{\text{SL}} \sum_{\sigma} \left(\varphi_{\mathbf{R}\mathbf{R}'}^* \chi_{\mathbf{R}\sigma}^\dagger \chi_{\mathbf{R}'\sigma} + c.c. \right) \right. \\ & + J_3^{\text{Weiss}} \sum_{\sigma} \left(\sigma m_{\mathbf{R}} \chi_{\mathbf{R}'\sigma}^\dagger \chi_{\mathbf{R}'\sigma} + \sigma m_{\mathbf{R}'} \chi_{\mathbf{R}\sigma}^\dagger \chi_{\mathbf{R}\sigma} \right) \\ & \left. + J_3^{\text{SL}} |\varphi_{\mathbf{R}\mathbf{R}'}|^2 - 2J_3^{\text{Weiss}} m_{\mathbf{R}} m_{\mathbf{R}'} \right]. \end{aligned} \quad (9)$$

In these expressions of \mathcal{L}_1 , \mathcal{L}_2 , and \mathcal{L}_3 , the sums over bonds \mathbf{R}, \mathbf{R}' are taken with the same connectivity as the couplings J_1 , J_2 , and J_3 respectively, which is indicated on figure 1: in \mathcal{L}_1 the bonds are nearest neighbors in two different planes P_n and P_{n+1} , in \mathcal{L}_2 the bonds are nearest neighbors in the same plane P_n , and in \mathcal{L}_3 the bonds are second nearest neighbors in the same plane. The convention used in these notations is that each pair $\mathbf{R}\mathbf{R}'$ is summed only once.

In the following, we will make some Ansatz for the mean-field parameters $m_{\mathbf{R}}$ and $\varphi_{\mathbf{R}\mathbf{R}'}$, which will generalize the approach of Ref. 21. This first requires to introduce space Fourier transforms and to use the momentum representation of the fermionic operators:

$$\chi_{\mathbf{k}\sigma} \equiv \frac{1}{\sqrt{N}} \sum_{\mathbf{R}} e^{-i\mathbf{k}\cdot\mathbf{R}} \chi_{\mathbf{R}\sigma}, \quad (10)$$

where N is the number of lattice sites. The inverse relation is

$$\chi_{\mathbf{R}\sigma} \equiv \frac{1}{\sqrt{N}} \sum_{\mathbf{k} \in \mathbf{BZ}_{\text{site}}^{\text{BCT}}} e^{i\mathbf{k}\cdot\mathbf{R}} \chi_{\mathbf{k}\sigma}. \quad (11)$$

Here, $\mathbf{BZ}_{\text{site}}^{\text{BCT}}$ refers to the first Brillouin zone of the BCT lattice of sites. This precision will be useful later since other

Brillouin zones will emerge from the dual lattices made of in-plane and interplane bonds (see appendix A). We define the mean-fields in reciprocal space as:

$$m_{\mathbf{k}} \equiv \frac{1}{\sqrt{N}} \sum_{\mathbf{R}} e^{-i\mathbf{k}\cdot\mathbf{R}} m_{\mathbf{R}}, \quad (12)$$

$$\varphi_{\mathbf{q}}^1 \equiv \frac{e^{i\theta_{\mathbf{q}}}}{2\sqrt{N}} \sum_n \sum_{\langle \mathbf{R}, \mathbf{R}' \rangle \in L_{n+1}} e^{-i\mathbf{q}\cdot\left(\frac{\mathbf{R}+\mathbf{R}'}{2}\right)} \varphi_{\mathbf{R}\mathbf{R}'}^*, \quad (13)$$

$$\varphi_{\mathbf{q}}^2 \equiv \frac{1}{\sqrt{2N}} \sum_n \sum_{\langle \mathbf{R}, \mathbf{R}' \rangle \in L_n} e^{-i\mathbf{q}\cdot\left(\frac{\mathbf{R}+\mathbf{R}'}{2}\right)} \varphi_{\mathbf{R}\mathbf{R}'}^*, \quad (14)$$

$$\varphi_{\mathbf{q}}^3 \equiv \frac{1}{\sqrt{2N}} \sum_n \sum_{\langle\langle \mathbf{R}, \mathbf{R}' \rangle\rangle \in L_n} e^{-i\mathbf{q}\cdot\left(\frac{\mathbf{R}+\mathbf{R}'}{2}\right)} \varphi_{\mathbf{R}\mathbf{R}'}^*. \quad (15)$$

Here, a phase factor $\theta_{\mathbf{q}} \equiv \mathbf{q} \cdot \mathbf{R}_0$ is introduced for the interlayer spin-liquid field $\varphi_{\mathbf{q}}^1$ in order to fix the origin of the interplane bond lattice at real space position $\mathbf{R}_0 \equiv (\mathbf{a} + \mathbf{b} + \mathbf{c})/4$. Such a global phase factors could be included arbitrarily for convenience to each mean-field. The site and bond dependence of the mean-fields can be recovered by the reciprocal Fourier relations:

$$m_{\mathbf{R}} \equiv \frac{1}{\sqrt{N}} \sum_{\mathbf{k} \in \text{BZ}_{\text{site}}^{\text{BCT}}} e^{i\mathbf{k}\cdot\mathbf{R}} m_{\mathbf{k}}, \quad (16)$$

and

$$\varphi_{\mathbf{R}\mathbf{R}'} = \begin{cases} \varphi_{\mathbf{R}\mathbf{R}'}^i & \text{if } \mathbf{R} \text{ and } \mathbf{R}' \text{ are connected by } J_i \\ 0 & \text{else,} \end{cases} \quad (17)$$

with

$$\varphi_{\mathbf{R}'\mathbf{R}}^1 \equiv \frac{1}{2\sqrt{N}} \sum_{\mathbf{q} \in \text{BZ}_{\text{bond}}^1} e^{i\mathbf{q}\cdot\left(\frac{\mathbf{R}+\mathbf{R}'}{2}\right) - i\theta_{\mathbf{q}}} \varphi_{\mathbf{q}}^1, \quad (18)$$

$$\varphi_{\mathbf{R}'\mathbf{R}}^2 \equiv \frac{1}{\sqrt{2N}} \sum_{\mathbf{q} \in \text{BZ}_{\text{bond}}^2} e^{i\mathbf{q}\cdot\left(\frac{\mathbf{R}+\mathbf{R}'}{2}\right)} \varphi_{\mathbf{q}}^2, \quad (19)$$

$$\varphi_{\mathbf{R}'\mathbf{R}}^3 \equiv \frac{1}{\sqrt{2N}} \sum_{\mathbf{q} \in \text{BZ}_{\text{bond}}^3} e^{i\mathbf{q}\cdot\left(\frac{\mathbf{R}+\mathbf{R}'}{2}\right)} \varphi_{\mathbf{q}}^3, \quad (20)$$

The different Brillouin zones emerging here from the dual lattices of bonds are defined and discussed in appendix A. At this general stage, the number of mean-field variables that can be considered is still huge. Concerning the Weiss mean-fields $m_{\mathbf{k}}$, we consider here magnetic structures described by a single- \mathbf{k} ordering wave-vector \mathbf{Q}_{AF} , excluding multi- \mathbf{k} structures. Hereafter, we will generalize this classical mean-field approach by doing similar Ansatz for the bond spin liquid mean-fields.

4. Mean-field Ansatz

Hereafter, the Weiss and spin liquid mean-fields are approximated using the following Ansatz:

$$m_{\mathbf{R}} = S_{\mathbf{Q}_{\text{AF}}} e^{i\mathbf{Q}_{\text{AF}}\cdot\mathbf{R}}, \quad (21)$$

$$\varphi_{\mathbf{R}\mathbf{R}'}^1 = \frac{1}{2} \left[\Phi_1 + i e^{i\mathbf{Q}\cdot\left(\frac{\mathbf{R}+\mathbf{R}'}{2}\right)} \Phi_{\mathbf{Q}} \right], \quad (22)$$

$$\varphi_{\mathbf{R}\mathbf{R}'}^2 = \Phi_2, \quad (23)$$

$$\varphi_{\mathbf{R}\mathbf{R}'}^3 = \Phi_3. \quad (24)$$

Here, $S_{\mathbf{Q}_{\text{AF}}}$ is the staggered magnetization characterizing an AF order. The wave-vector ordering \mathbf{Q}_{AF} will be fixed by minimization of the spin-wave spectrum resulting from the Weiss field. The three fields Φ_1 , Φ_2 , and Φ_3 correspond to the homogeneous parts of the spin liquid terms along the three kinds of bonds that are considered here. The emergence of three such homogeneous spin liquid fields is a natural BCT lattice generalization of the RVB decoupling introduced initially on triangular lattice²⁴ and later on a square lattice.^{25,26} The extra term $\Phi_{\mathbf{Q}}$ included in this Ansatz takes into account a possible spatial modulation of the spin liquid field. The specific choice of this spin-liquid modulation is motivated by previous work of Ref. 21, where only the interplane spin-liquid term $\varphi_{\mathbf{R}\mathbf{R}'}^1$ was considered. This modulation is defined on the bond lattice by a wave-vector \mathbf{Q} , and it can lower the lattice translation symmetry. Invoking the momentum representation given by Eqs. (12, 13, 14, 15), the mean-field Ansatz Eqs. (21, 22, 23, 24) can be expressed as

$$m_{\mathbf{k}} = S_{\mathbf{Q}_{\text{AF}}} \sqrt{N} \delta(\mathbf{k} - \mathbf{Q}_{\text{AF}}), \quad (25)$$

$$\varphi_{\mathbf{q}}^1 = \Phi_1 \sqrt{N} \delta(\mathbf{q}) + \Phi_{\mathbf{Q}} \sqrt{N} \delta(\mathbf{q} - \mathbf{Q}), \quad (26)$$

$$\varphi_{\mathbf{q}}^2 = \Phi_2 \sqrt{2N} \delta(\mathbf{q}), \quad (27)$$

$$\varphi_{\mathbf{q}}^3 = \Phi_3 \sqrt{2N} \delta(\mathbf{q}), \quad (28)$$

where $\delta(\mathbf{q})$ denotes the Dirac distribution. We also assume an homogeneous and constant Lagrange multiplier $\lambda_{\mathbf{R}} = \lambda_0$. Finally, within this mean-field Ansatz, the Lagrangian (7) can be expressed explicitly in terms of the \mathbf{k} -dependent fermions as

$$\begin{aligned} \mathcal{L} = & \sum_{\sigma\mathbf{k}} \chi_{\mathbf{k}\sigma}^\dagger (\partial_\tau + \lambda_0) \chi_{\mathbf{k}\sigma} + N \lambda_0 \\ & + 4J_1^{\text{SL}} \Phi_1 \sum_{\sigma\mathbf{k}} \gamma_{1,\mathbf{k}} \chi_{\mathbf{k}\sigma}^\dagger \chi_{\mathbf{k}\sigma} + N J_1^{\text{SL}} (|\Phi_1|^2 + |\Phi_{\mathbf{Q}}|^2) \\ & + 2J_1^{\text{SL}} e^{-i\theta_{\mathbf{Q}}} \Phi_{\mathbf{Q}} \sum_{\sigma\mathbf{k}} \gamma_{\mathbf{Q},\mathbf{k}} \left[\chi_{\mathbf{k}\sigma}^\dagger \chi_{\mathbf{k}+\mathbf{Q},\sigma} + c.c. \right] \\ & + 2J_2^{\text{SL}} \Phi_2 \sum_{\sigma\mathbf{k}} \gamma_{2,\mathbf{k}} \chi_{\mathbf{k}\sigma}^\dagger \chi_{\mathbf{k}\sigma} + 2N J_2^{\text{SL}} |\Phi_2|^2 \\ & + 4J_3^{\text{SL}} \Phi_3 \sum_{\sigma\mathbf{k}} \gamma_{3,\mathbf{k}} \chi_{\mathbf{k}\sigma}^\dagger \chi_{\mathbf{k}\sigma} + 2N J_3^{\text{SL}} |\Phi_3|^2 \\ & + \sum_{\sigma\mathbf{k}} \sigma J_{\mathbf{Q}_{\text{AF}}} S_{\mathbf{Q}_{\text{AF}}} \chi_{\mathbf{k}\sigma}^\dagger \chi_{\mathbf{k}+\mathbf{Q}_{\text{AF}},\sigma} - N J_{\mathbf{Q}_{\text{AF}}} |S_{\mathbf{Q}_{\text{AF}}}|^2, \end{aligned} \quad (29)$$

where the effective spin-wave dispersion is

$$J_{\mathbf{Q}_{\text{AF}}} \equiv 8J_1^{\text{Weiss}} \gamma_{1,\mathbf{Q}_{\text{AF}}} + 2J_2^{\text{Weiss}} \gamma_{2,\mathbf{Q}_{\text{AF}}} + 4J_3^{\text{Weiss}} \gamma_{3,\mathbf{Q}_{\text{AF}}}, \quad (30)$$

and the effective dispersions resulting from the spin-liquid decoupling are given by:

$$\gamma_{1,\mathbf{k}} \equiv \cos\left(\frac{k_x a}{2}\right) \cos\left(\frac{k_y a}{2}\right) \cos\left(\frac{k_z c}{2}\right), \quad (31)$$

$$\gamma_{\mathbf{Q},\mathbf{k}} \equiv \gamma_{1,\mathbf{k}+\mathbf{Q}/2}, \quad (32)$$

$$\gamma_{2,\mathbf{k}} \equiv \cos(k_x a) + \cos(k_y a), \quad (33)$$

$$\gamma_{3,\mathbf{k}} \equiv \cos(k_x a) \cos(k_y a). \quad (34)$$

The values considered for \mathbf{Q}_{AF} will be those that minimize the spin-wave dispersion $J_{\mathbf{Q}_{\text{AF}}}$. Hereafter, we will restrict the analysis to some specific modulating vectors \mathbf{Q} in $\mathbf{BZ}_{\text{bond}}^1$ that are equivalent to \mathbf{Q}_{AF} in $\mathbf{BZ}_{\text{site}}^{\text{BCT}}$ (definitions of the various Brillouin zones are discussed in appendix A). One key assumption that will be made in the following is that we will consider only breaking of symmetries that lead to commensurate order with doubling of the unit cell. This restrictive but realistic assumption has a crucial simplifying consequence: $2\mathbf{Q}$, $\mathbf{Q} + \mathbf{Q}_{\text{AF}}$, and $2\mathbf{Q}_{\text{AF}}$ are all equivalent to $\mathbf{0}$. In the Lagrangian, the MSL and AF terms correlate fermions of momentum \mathbf{k} with fermions of momenta $\mathbf{k} + \mathbf{Q}$ and $\mathbf{k} + \mathbf{Q}_{\text{AF}}$. Therefore, there is no new harmonics generated by these interactions since the second harmonics would correlate momenta $\mathbf{k} + \mathbf{Q}$ and $\mathbf{k} + \mathbf{Q}_{\text{AF}}$ with \mathbf{k} . There could be more possible solutions obtained by considering non-equivalent \mathbf{Q} and \mathbf{Q}_{AF} , but such solutions would correspond to a lowering of the lattice symmetry associated to a bigger unit cell made of more than two atoms.

5. Free energy functional

Invoking the assumptions $\mathbf{Q} = \mathbf{Q}_{\text{AF}}$ and $2\mathbf{Q}_{\text{AF}} = \mathbf{0}$, the free energy can be expressed from the mean-field Lagrangian Eq. (29) as

$$\begin{aligned} F(\alpha_1, \alpha_2, \alpha_3, \lambda_0, \Phi_1, \Phi_{\mathbf{Q}}, \Phi_2, \Phi_3, S_{\mathbf{Q}_{\text{AF}}}) = \\ - \frac{k_B T}{2N} \sum_{\mathbf{k} \in \mathbf{BZ}_{\text{site}}^{\text{BCT}}} \sum_{\sigma, s = \pm} \ln\left(1 + e^{-\beta \Omega_{\mathbf{k}}^s}\right) - \lambda_0 - J_{\mathbf{Q}_{\text{AF}}} |S_{\mathbf{Q}_{\text{AF}}}|^2 \\ + J_1^{\text{SL}} (|\Phi_1|^2 + |\Phi_{\mathbf{Q}}|^2) + 2J_2^{\text{SL}} |\Phi_2|^2 + 2J_3^{\text{SL}} |\Phi_3|^2. \end{aligned} \quad (35)$$

where the eigenenergies involved are given by

$$\begin{aligned} \Omega_{\mathbf{k}}^{\pm} = \lambda_0 + 2J_2^{\text{SL}} \gamma_{2,\mathbf{k}} \Phi_2 + 4J_3^{\text{SL}} \gamma_{3,\mathbf{k}} \Phi_3 \\ \pm \sqrt{(J_{\mathbf{Q}_{\text{AF}}})^2 |S_{\mathbf{Q}_{\text{AF}}}|^2 + 16(J_1^{\text{SL}})^2 [(\gamma_{1,\mathbf{k}})^2 |\Phi_1|^2 + (\gamma_{\mathbf{Q},\mathbf{k}})^2 |\Phi_{\mathbf{Q}}|^2]} \end{aligned} \quad (36)$$

The explicit dependence of the free energy in terms of the variational decoupling fields α_1 , α_2 , and α_3 is obtained from the definition Eq. (2) by identifying $J_i^{\text{Weiss}} = J_i \cos^2(\alpha_i)$ and $J_i^{\text{SL}} = J_i \sin^2(\alpha_i)$. The Weiss field and spin liquid dispersion terms are given by Eqs. (30, 31, 32, 33, 34). The mean-field and variational parameters correspond to the minima of the free energy.

	α_1	α_2
Case A	0 or $\pi/2$	0 or $\pi/2$
Case B	0 or $\pi/2$	free parameter
Case C	free parameter	0 or $\pi/2$
Case D	free parameter	free parameter

TABLE I. Characteristics of the four possible cases for the variational decoupling parameters α_1 and α_2 .

III. TEMPERATURE PHASE DIAGRAM FOR $J_3 = 0$

Before analyzing the ground state of the J_1 - J_2 - J_3 model, we start with the simplified situation where $J_3 = 0$. In this section we are thus not concerned with the fields α_3 and Φ_3 . Hereafter, we use the reduced notation $\mathbf{Q} \equiv (h, k, l)$ for the ordering wave-vectors $\mathbf{Q} = 2\pi(h/a, k/a, l/c)$. When stable, all magnetic phases are analyzed for the wave vectors $\mathbf{Q}_{\text{AF}}^{\text{I}} = (1, 1, 1)$ and $\mathbf{Q}_{\text{AF}}^{\text{II}} = (1/2, 1/2, 0)$, that correspond to the classical magnetic solution, i.e., with $\alpha_1 = \alpha_2 = 0$. Experimental examples of these two kinds of classical Néel orders in BCT lattices are realized in the AF phases of URu_2Si_2 and cuprates for $\mathbf{Q}_{\text{AF}}^{\text{I}}$ and $\mathbf{Q}_{\text{AF}}^{\text{II}}$, respectively.

A. Method of calculation for $J_3 = 0$

In order to find the stable configuration for the $J_3 = 0$ case, we have to minimize the free energy functional Eq. (35). It is first minimized as much as possible analytically as a function of the variational decoupling fields α_1 and α_2 . To do this, we start by expressing the seven saddle point relations for $F(\alpha_1, \alpha_2, \lambda_0, \Phi_1, \Phi_{\mathbf{Q}}, \Phi_2, S_{\mathbf{Q}_{\text{AF}}})$. The resulting system of equations is detailed in appendix C, and invokes several formal sums over momenta \mathbf{k} . After non trivial but straightforward algebraic transformations this system can be rewritten as seven equations (C13-C19) that involve five independent sums over \mathbf{k} . Explicit expressions of these five sums are given in Eqs. (C8-C12). The resolution of this system in general requires a numerical approach, but we also find some trivial solutions that may have a physical meaning. Hereafter we analyze more precisely the trivial solutions that are obtained when the variational decoupling parameters α_1 and α_2 take the extreme values 0 or $\pi/2$. Physically, such trivial solutions correspond to decoupling the corresponding Heisenberg interaction term (with J_1 or with J_2) in a pure channel that is either Weiss or spin-liquid. Hereafter, we analyze the possible solutions by considering the four different cases as defined in table I:

1. Case A

Here, we consider extreme values for α_1 and α_2 so that $\sin(2\alpha_1) = \sin(2\alpha_2) = 0$. The saddle point equations (C13) and (C14) are thus trivially satisfied and we are left with Eqs. (C15-C19). Among these five remaining equations, some

may also be satisfied trivially.

The sub-case $(\alpha_1, \alpha_2) = (0, 0)$ corresponds to the classical mean Weiss field approximation. The two possible antiferromagnetic ground states compete, characterized respectively by the ordering wave-vectors $\mathbf{Q}_{\text{AF}}^{\text{I}}$ and $\mathbf{Q}_{\text{AF}}^{\text{II}}$. The corresponding temperature-coupling classical phase diagram is depicted in figure 3 as a function of the dimensionless parameters T/J_1 and J_2/J_1 . The classical phase transition between these two kinds of AF orders is realized at finite temperature when $J_1 = J_2$.

The sub-case $(\alpha_1, \alpha_2) = (0, \pi/2)$ does not correspond to a physically realistic situation. Indeed, decoupling J_1 in the pure Weiss and J_2 in the pure spin liquid channels artificially bypasses the underlying frustration problem. Such a solution artificially induces ferromagnetic planes coupled antiferromagnetically among them: this is compatible with J_1 interaction. But the inplane spin liquid term Φ_2 vanishes, leading to a J_2 -independent unphysical solution. It will not be considered in the following.

For $(\alpha_1, \alpha_2) = (\pi/2, 0)$, the interplane SL field competes with the inplane magnetization Weiss field with $\mathbf{Q}_{\text{AF}}^{\text{II}} = (1/2, 1/2, 0)$. Here, since we restrict our analysis to commensurate orders with at most a doubling of the unit cell, we enforce $\Phi_{\mathbf{Q}} = 0$. The phase diagram presents a pure homogeneous SL solution with only Φ_1 non-zero for $J_2/J_1 \lesssim 0.3$, and a purely magnetic solution is recovered for $J_2/J_1 > 0.5$. But these two extreme situations are more appropriately described by taking (α_1, α_2) equal to $(\pi/2, \pi/2)$ and $(0, 0)$ respectively. A more interesting solution is found in the range $0.3 \lesssim J_2/J_1 \lesssim 0.5$, where the homogeneous SL field Φ_1 coexists with the inplane antiferromagnetic order. Nevertheless, in this regime of parameters, the magnetic order obtained with $(\alpha_1, \alpha_2) = (0, 0)$ has a much lower energy. Therefore, in the following we will not consider the sub-case $(\alpha_1, \alpha_2) = (\pi/2, 0)$.

The last trivial sub-case is $(\alpha_1, \alpha_2) = (\pi/2, \pi/2)$, corresponding to pure spin-liquid decoupling. Here, the interplane MSL phase competes with the intraplane SL phase. For $J_2 < J_1$, the MSL is predominant. Comparing the values of the free energy obtained by considering three possible ordering wave vectors $(1, 1, 1)$, $(0, 0, 1)$, and $(1, 0, 0)$, we found that $\mathbf{Q} = (1, 1, 1)$ corresponds to the most stable MSL state. For $J_2 \gtrsim J_1$ the intraplane SL takes place. The temperature-coupling phase diagram for this sub-case is depicted in figure 4. Due to the lattice breaking of symmetry associated with the MSL field, the critical line $T_{\Phi_{\mathbf{Q}}}$ indicates a true phase transition that would survive beyond the mean-field. The other mean-field critical temperature T_{Φ_2} rather describes a crossover since the inplane spin-liquid field Φ_2 here is homogeneous.

2. Case B

In this case, the saddle point condition (C14) can be simplified as $\gamma_{2, \mathbf{Q}_{\text{AF}}} |S_{\mathbf{Q}_{\text{AF}}}|^2 + |\Phi_2|^2 = 0$. Letting aside the trivial high temperature solution where both $S_{\mathbf{Q}_{\text{AF}}}$ and Φ_2 vanish, we consider here only the magnetic wave vector $\mathbf{Q}_{\text{AF}}^{\text{II}}$. Indeed

Eq. (33) gives $\gamma_{2, \mathbf{Q}_{\text{AF}}^{\text{I}}} > 0$ but $\gamma_{2, \mathbf{Q}_{\text{AF}}^{\text{II}}} < 0$. Here, as a consequence of relation (C14), the intraplane spin liquid field Φ_2 is proportional to the local magnetization. Solving the remaining saddle point equations in the sub-case $\alpha_1 = 0$, we find the numerical value $\sin^2(\alpha_2) = 0.675 \pm 0.01$. For the other sub-case, $\alpha_1 = \pi/2$, the pure MSL state has the most stable configuration until $J_2 \lesssim 2J_1$, then the pure inplane solution with non zero $S_{\mathbf{Q}_{\text{AF}}}$ and Φ_2 is present for higher J_2 .

3. Case C

Here, excluding the extreme solutions for α_1 , the saddle point Eq. (C13) is simplified as $8\gamma_{1, \mathbf{Q}_{\text{AF}}} |S_{\mathbf{Q}_{\text{AF}}}|^2 + |\Phi_1|^2 + |\Phi_{\mathbf{Q}}|^2 = 0$. In this case, Eq. (31) gives $\gamma_{1, \mathbf{Q}_{\text{AF}}^{\text{I}}} < 0$ but $\gamma_{1, \mathbf{Q}_{\text{AF}}^{\text{II}}} > 0$. Therefore, only the ordering wave-vector $\mathbf{Q}_{\text{AF}}^{\text{I}}$ is considered for the magnetic phase. The trivial solution with vanishing $S_{\mathbf{Q}_{\text{AF}}}$, Φ_1 , and $\Phi_{\mathbf{Q}}$ is not considered here, and we thus focus on the phases where magnetic order coexist with interlayer spin-liquid fields. For the first sub-case $\alpha_2 = 0$ we naturally explore the situation with $\Phi_2 = 0$. But for $\alpha_2 = \pi/2$ all the competing mean-fields may coexist. Typically, this sub-case has similarities with the pure spin-liquid one discussed above and illustrated by figure 4: the parameter J_1/J_2 tunes the competition between the interlayer MSL order and the inplane SL. However, here, a non-zero MSL field must coexist with a non-zero local magnetization field.

4. Case D

This case is in principle the most general one since it corresponds to non extreme values of both α_1 and α_2 . Nevertheless, this situation can not be realized and it would correspond to all mean-fields vanishing. Indeed, assuming that neither α_1 nor α_2 are extreme, the saddle point relations (C13) and (C14) give $8\gamma_{1, \mathbf{Q}_{\text{AF}}} |S_{\mathbf{Q}_{\text{AF}}}|^2 + |\Phi_1|^2 + |\Phi_{\mathbf{Q}}|^2 = 0$ and $\gamma_{2, \mathbf{Q}_{\text{AF}}} |S_{\mathbf{Q}_{\text{AF}}}|^2 + |\Phi_2|^2 = 0$. Non zero solutions for the mean-field parameters would thus require an ordering wave-vector \mathbf{Q}_{AF} such that both $\gamma_{1, \mathbf{Q}_{\text{AF}}} < 0$ and $\gamma_{2, \mathbf{Q}_{\text{AF}}} < 0$. Since these two conditions cannot be realized simultaneously, neither by $\mathbf{Q}_{\text{AF}}^{\text{I}}$ nor by $\mathbf{Q}_{\text{AF}}^{\text{II}}$, we exclude case D from our study.

B. Results for $J_3 = 0$

All possible cases described above are studied by solving numerically the saddle point equations given in appendix C. We computed the free energy for each case, as functions of J_2/J_1 and T/J_1 . For a sake of clarity, figure 2 shows its evolution at $T = 0$ only. The finite T results are not presented here but they do not exhibit any extra free energy "crossing" between these cases.

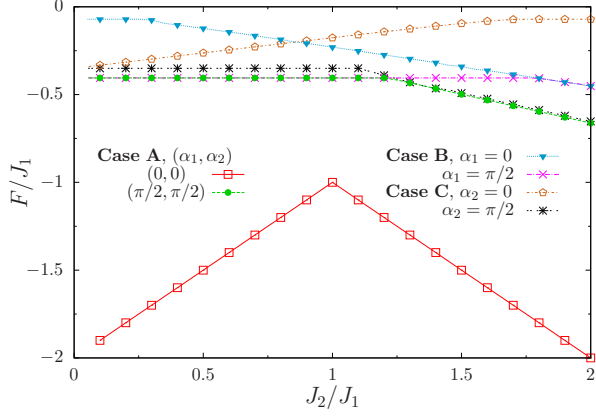


FIG. 2. Ground state energy of the model computed with $J_3 = 0$ as a function of J_2/J_1 for the various relevant cases discussed in this work and defined in table I.

The main result that emerges here from our variational approach for $J_3 = 0$ is the following: among all the considered cases, the classical purely AF mean-field solutions obtained with $\alpha_1 = \alpha_2 = 0$ are always the most stable ones. The second most stable family of solutions are obtained with pure spin-liquid decoupling channels $\alpha_1 = \alpha_2 = \pi/2$. All the other combinations are found to be energetically less favorable. Here, we describe the two phase diagrams obtained for these two variational sub-cases. The temperature-coupling phase diagrams for both configurations $\alpha_1 = \alpha_2 = 0$ and $\alpha_1 = \alpha_2 = \pi/2$ are shown in figures 3 and 4 respectively.

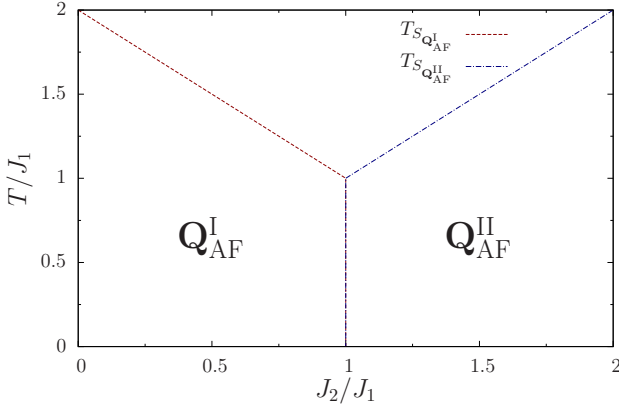


FIG. 3. Temperature-coupling phase diagram obtained with the purely magnetic configuration $\alpha_1 = \alpha_2 = 0$ for $J_3 = 0$. The lines indicate the Néel ordering temperatures of the two magnetic orders corresponding to $\mathbf{Q}_{\text{AF}}^{\text{I}} = (1, 1, 1)$ and $\mathbf{Q}_{\text{AF}}^{\text{II}} = (1/2, 1/2, 0)$.

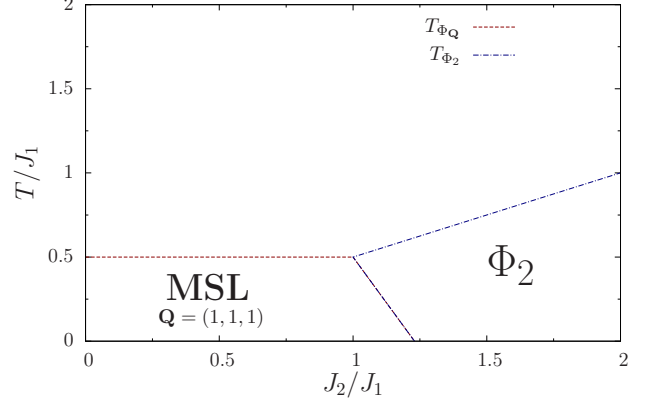


FIG. 4. Temperature-coupling phase diagram obtained with the purely spin-liquid decoupling channels $\alpha_1 = \alpha_2 = \pi/2$ for $J_3 = 0$. The lines indicate the critical temperatures below which the corresponding mean-field Φ_1 , Φ_2 , and $\Phi_{\mathbf{Q}}$ are non-zero. Among these lines, $T_{\Phi_1} = T_{\Phi_{\mathbf{Q}}}$ is still expected to indicate a transition beyond the mean field because $\Phi_{\mathbf{Q}}$ is associated to a lattice symmetry breaking. T_{Φ_2} is expected to mark a crossover beyond the mean-field.

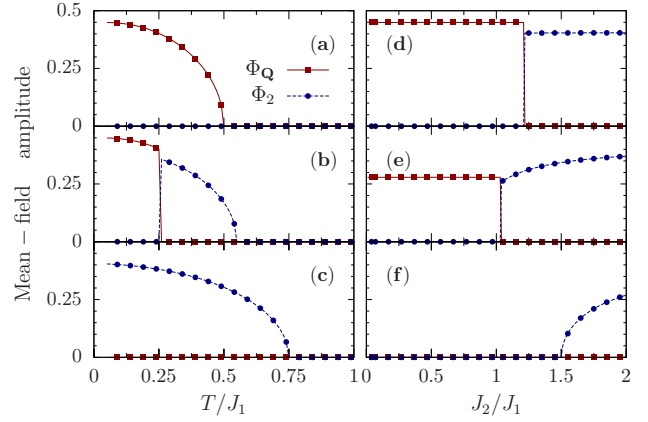


FIG. 5. Amplitude of the SL mean-field parameters $\Phi_{\mathbf{Q}}$ and Φ_1 (red squares) and Φ_2 (blue circles) computed for $J_3 = 0$ and $\alpha_1 = \alpha_2 = \pi/2$. Left: as a function of temperature for fixed $J_2/J_1 = 0.5$ (a), 1.1 (b), 1.5 (c). Right: as a function of J_2/J_1 for fixed temperature $T/J_1 = 0.05$ (d), 0.4 (e), 0.75 (f). With numerical accuracy we find $\Phi_1 = \Phi_{\mathbf{Q}}$.

While the purely AF solutions are the most stable the purely SL ones are energetically very close. Any mixed solution where both Weiss and SL mean-fields would coexist is found to be much less favorable and can also be excluded. Therefore, we can deduce that any fluctuation that would destabilize the AF order leave some room for stabilizing a pure SL phase. We also find that the SL parameters $\Phi_1 = \Phi_{\mathbf{Q}}$ and Φ_2 do not coexist, as illustrated by figure 5. Depending on the value of J_2/J_1 , there are three different kinds of temperature behaviors, corresponding to cases *a*, *b*, and *c*. Furthermore, we remark that the transition between the Modulated and the Φ_2 -dominated SL phases is characterized by a discontinuity of the corresponding mean-fields. This feature is in contrast with the continuous vanishing of these fields at the crit-

ical temperature separating the paramagnetic fully-decoupled phase from the SL ones. We thus conclude that the MSL transition is second order for $J_2 < J_1$ and becomes first order for $J_2 > J_1$. The transition temperature T_{Φ_2} is expected to indicate a crossover between the paramagnetic high T and the SL low T regimes when fluctuations beyond the mean-field approximation are included. Indeed, Φ_2 is not associated to any breaking of symmetry. But we expect the transition at T_{Φ_Q} to survive beyond the mean-field since the MSL phase is characterized by a breaking of lattice symmetry.

An interesting feature also appears for the MSL solution: with a relatively high numerical accuracy the modulation field Φ_Q is found to be always equal to the homogeneous field Φ_1 . Invoking the Ansatz Eq. (22), this leads to a very extreme situation for the inter-layer field $\varphi_{\mathbf{R}\mathbf{R}'}^1 = \frac{1}{2}[\Phi_1 \pm \Phi_Q]$ which vanishes on half of the bonds while it keeps the finite value $\Phi_1 = \Phi_Q$ on the other bonds. Introducing the probability $p_{\mathbf{R}\mathbf{R}'}^{singlet}$ that a given bond $\mathbf{R}\mathbf{R}'$ forms a singlet (see Appendix B), the formation of the MSL state can be interpreted here as follows: first, the interaction terms for all the inter-layer bonds such that $\mathbf{Q} \cdot (\mathbf{R} + \mathbf{R}')/2 = \pi/2$ are effectively decoupled at the mean-field level, leading to a local probability $p_{\mathbf{R}\mathbf{R}'}^{singlet} = 1/4$ and a vanishing spin-spin correlations $\langle \vec{S}_{\mathbf{R}} \cdot \vec{S}_{\mathbf{R}'} \rangle = 0$. Then the spin-liquid with $\langle \vec{S}_{\mathbf{R}} \cdot \vec{S}_{\mathbf{R}'} \rangle \neq 0$ is formed on the other inter-layer bonds, with $\mathbf{Q} \cdot (\mathbf{R} + \mathbf{R}')/2 = -\pi/2$, that remain effectively coupled. Using the numerical value $\Phi_1 = \Phi_Q \approx 0.45$ computed at $T = 0$ in the MSL (see figure 5), and invoking expression Eq. (B4), we find that the singlet probability on these effectively coupled bonds is $p_{\mathbf{R}\mathbf{R}'}^{singlet} \approx 0.60$. This value is, not surprisingly, higher than $1/4$, and it has to be compared with the value $\ln(2) \approx 0.69$ that is predicted for a one-dimensional Heisenberg chain using exact methods like Bethe Ansatz³⁵ or numerical renormalization technics.³⁶ We may thus interpret the MSL as a crystal of interacting filaments formed by the connected effectively coupled bonds. In this picture, spin excitations are deconfined fermions moving along the filaments. This may generalize the usual concept of valence bond crystal where localized spin 1 excitations correspond to confined fermions.

IV. MEAN-FIELD GROUND STATE OF THE J_1 - J_2 - J_3 MODEL

Here we analyze the ground state of the J_1 - J_2 - J_3 model within the mean-field Ansatz described above. In the previous section it was shown that for $J_3 = 0$ the low temperature most stable configuration is obtained by choosing purely magnetic Weiss mean-field decoupling channels. The second most stable solution corresponds to the purely spin liquid decoupling channels. Here, we assume that this result can be extended to the decoupling of the intraplane next nearest neighbor interaction J_3 . We therefore assume that α_3 can take only the extreme values 0 or $\pi/2$.

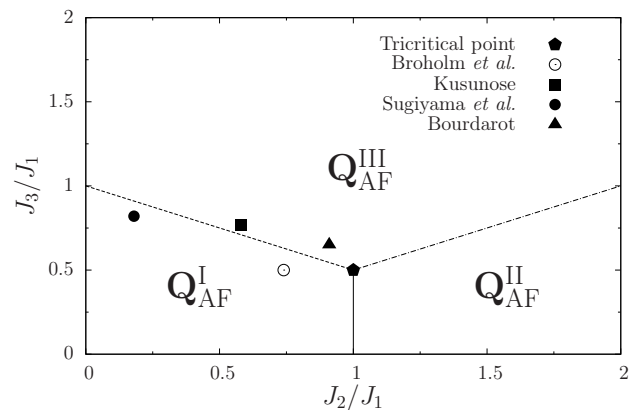


FIG. 6. Phase diagram characterizing the ground state of the J_1 - J_2 - J_3 model obtained within the pure Weiss mean-field decoupling channels $\alpha_1 = \alpha_2 = \alpha_3 = 0$. Three different magnetic orders are found, characterized by the wave-vectors \mathbf{Q}_{AF}^I , \mathbf{Q}_{AF}^{II} and \mathbf{Q}_{AF}^{III} . We name *magnetic tricritical point* the highly degenerate point corresponding to the crossing of the three critical lines. Additionally, we include four points obtained from various fits of inelastic neutron scattering (INS) data on URu_2Si_2 : from Broholm *et al.*,³⁷ Kusunose *et al.*,³⁸ Sugiyama *et al.*³⁹ and Bourdarot.⁴⁰

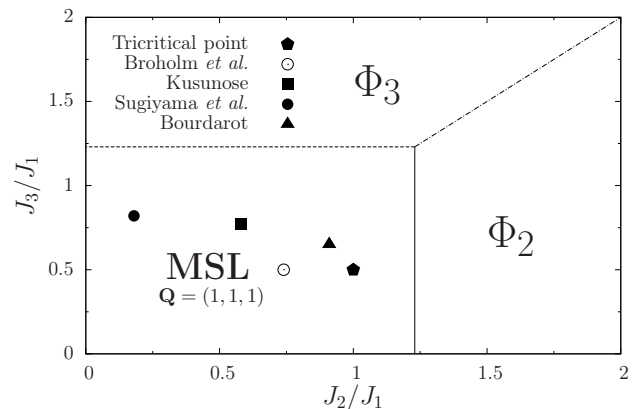


FIG. 7. Phase diagram characterizing the ground state of the J_1 - J_2 - J_3 model obtained within the pure spin-liquid mean-field decoupling channels $\alpha_1 = \alpha_2 = \alpha_3 = \pi/2$. The MSL phase corresponds to finite Φ_1 and Φ_Q . The two other spin-liquid phases correspond to a vanishing Φ_Q and finite values of the nearest and next nearest neighbor inplane spin liquid fields Φ_2 and Φ_3 respectively. Among the three critical lines depicted here, only the ones indicating the MSL phase would still correspond to a transition when considering fluctuations beyond the mean-field approximation. The magnetic tricritical point is defined as the highly degenerate point in the purely magnetic phase diagram. The additional points obtained from INS data are included here with the same notations as in figure 6.

Solving numerically the two extreme cases, we find that, at the mean-field level, the classical magnetic solution with $\alpha_1 = \alpha_2 = \alpha_3 = 0$ is the most stable variational configuration. The resulting ground state phase diagram is presented in figure 6 as a function of the dimensionless parameters J_2/J_1 and J_3/J_1 . Three possible ordering wave-vectors are obtained, $\mathbf{Q}_{AF}^I = (1, 1, 1)$, $\mathbf{Q}_{AF}^{II} = (1/2, 1/2, 0)$,

or $\mathbf{Q}_{\text{AF}}^{\text{III}} = (1/2, 0, 0)$, that correspond to the three different regimes where the Weiss field can be dominated by J_1 , J_2 , or J_3 respectively. A highly degenerate point is found for $J_1 = J_3 = 2J_2$, that we name *magnetic tricritical point*.

Figure 7 depicts the phase diagram obtained within a purely spin-liquid mean-field decoupling $\alpha_1 = \alpha_2 = \alpha_3 = \pi/2$. At the mean-field level we find three different phases, that are characterized by finite values of $\Phi_{\mathbf{Q}}$, Φ_2 , or Φ_3 . Beyond the mean-field, we expect that only the critical line defining finite $\Phi_{\mathbf{Q}}$ would still correspond to a phase transition, associated with a translation symmetry breaking. We remark that the MSL solution that we obtain corresponds to $\Phi_1 = \Phi_{\mathbf{Q}}$, and it corresponds to the formation of a crystal of connected filaments as described above.

The position of the magnetic tricritical point is also indicated in the pure spin liquid phase diagram, figure 7. It is very surprising to see that this point which is highly degenerate from a Weiss mean-field perspective turns to be located well inside the MSL phase. Several earlier works have been dedicated to the characterization of the magnetic ground state of a frustrated Heisenberg model on a square lattice,^{41–43} that can be realized here for $J_1 = 0$. It was shown that quantum fluctuations can stabilize a non magnetic spin-liquid phase between the antiferromagnetic phases $\mathbf{Q}_{\text{AF}}^{\text{I}}$ and $\mathbf{Q}_{\text{AF}}^{\text{III}}$. For this reason, we expect that huge quantum fluctuations of the Weiss mean-field should occur around all the critical lines separating the three possible phases $\mathbf{Q}_{\text{AF}}^{\text{I}}$, $\mathbf{Q}_{\text{AF}}^{\text{II}}$, and $\mathbf{Q}_{\text{AF}}^{\text{III}}$. The position of the magnetic tricritical point inside the MSL phase suggests that the fluctuations of the MSL mean-field should be much less critical. Therefore, we expect that fluctuations beyond the mean-field will destabilize the magnetic solutions around all their degeneracy lines. We believe that the MSL mean-field solution should be more robust for all the regions that are sufficiently far from the MSL critical line. This is the case, for example, of the area around the magnetic tricritical point.

V. DISCUSSION AND APPLICATIONS TO MATERIALS WITH BCT STRUCTURE

A. Relevance for Hidden order in URu₂Si₂

The HO phase in URu₂Si₂ cannot be explained by the formation of too tiny local magnetic moments. Nevertheless, there are strong experimental evidences that the thermodynamic anomaly measured at the transition⁴⁴ has a magnetic origin. For example, the HO phase is characterized by a peak revealed by Inelastic Neutron Scattering (INS) at the commensurate wave-vector $\mathbf{Q}_{\text{AF}} = (1, 0, 0)$ in reduced notation.^{45–47} This wave-vector is surprisingly identical to the one that describes the pressure-induced AF phase of this compound. In the BCT structure, this AF order represents a ferromagnetic correlation in the **a**, **b** directions (see Fig. 1), with antiferromagnetic correlations between nearest (**a**, **b**) planes. Recently, it was proposed that a quantum modulated spin liquid (MSL) phase could be stabilized by frustration and explain the origin of the hidden order phase in URu₂Si₂.^{20–22} A phase with a similar order as the MSL has also been proposed

in terms of unconventional spin-orbital density wave,^{48–50} where the order parameter characterizes a spatial commensurate modulation of the intersite hybridization between 5f states.

The first Heisenberg model on a BCT lattice that was proposed for URu₂Si₂ was introduced by Broholm *et al.*,³⁷ trying to fit INS data in terms of spin density wave (SDW) excitations from an AF ground state. As we will see further, the resulting SDW model obtained by Broholm corresponds to a highly frustrated situation. The SDW scenario has later been contradicted by several other experiments. Nonetheless, the classical version of a J_1 - J_2 - J_3 Heisenberg model has been proposed by Sugiyama *et al.*^{39,51} as a frustration scenario to explain the cascade of metamagnetic-like transitions and magnetization plateaux that are observed in URu₂Si₂. More recently, INS data analysis was invoked by Kusunose who proposed a competition between multipolar and AF Ising-like orders as a scenario for the HO-AF pressure-induced transition.³⁸ Bourdarot also recently proposed numerical values for J_1 , J_2 and J_3 in order to fit his INS data.⁴⁰

We are aware that modeling URu₂Si₂ with the present J_1 - J_2 - J_3 quantum Heisenberg model may constitute a very crude approximation with respect to several aspects: for example, the real system is metallic, and also, local 5f electronic states require an Ising-like highly anisotropic multiplet description. Nevertheless, the numerous previous attempts to fit INS data using effective SDW dispersions make it worth checking where the fitted parameter would locate URu₂Si₂ on the mean-field phase diagrams we analyzed here.

Hereafter, we use four different fits of various INS datas: the original fit introduced by Broholm *et al.* in Ref.,³⁷ the fit introduced more recently by Kusunose³⁸ from Broholm's datas, the fit of INS datas from Sugiyama *et al.*,^{39,51} and the one from Bourdarot's data.⁴⁰ These fits invoke not only J_1 - J_2 - J_3 terms but also up to seven Heisenberg-like interaction parameters in the BCT structure. Neglecting these extra parameters, we extracted the numerical values of J_1 , J_2 and J_3 provided by each fit. The corresponding dimensionless pairs of ratios J_2/J_1 and J_3/J_1 thus provide specific points in the phase diagrams as indicated on figures 6 and 7. The absolute numerical values of J_1 , J_2 and J_3 that were provided by these four different fits do not coincide. This quantitative difference between fits is easily understandable: different experimental INS data were involved, and different extra fitting parameters were also involved, that we have not considered here. Nevertheless, it is remarkable that the four different fits all provide antiferromagnetic values for J_1 , J_2 , and J_3 . Furthermore, the most interesting observation is the following: all of these different fits locate URu₂Si₂ in the very close vicinity of the transition line separating the two ordered states $\mathbf{Q}_{\text{AF}}^{\text{I}}$ and $\mathbf{Q}_{\text{AF}}^{\text{III}}$, as indicated on figure 6. We thus expect frustration to be very important as also noticed by Sugiyama *et al.*,^{39,51} and spin fluctuations may destabilize the magnetically ordered phase. Considering now the spin-liquid phase diagram on figure 7, we find that the four points that correspond to the different fits of INS data are all located well inside the MSL phase.

This observation together with the analysis presented here suggest the MSL scenario as an alternative to the geometri-

cal frustration problem that seems to prevent URu_2Si_2 from forming an AF order: the pressure induced HO-AF transition which is observed in this compound at low temperature could be mostly controlled by the tuning of J_3/J_1 . At ambient pressure, quantum fluctuations are too strong and only the MSL state is realized. Applying pressure pushes the system away from the critical line, reducing the fluctuations and thus stabilizing the AF state with wave-vector ordering $\mathbf{Q}_{\text{AF}}^{\text{I}}$.

We are aware that this scenario should be completed by including charge fluctuation effects and by taking into account the precise $5f$ local multiplet structure at the origin of the magnetic ordering. We believe that the concept of spatially modulated highly entangled state which emerges here from frustration would survive when adding such sophistications to the J_1 - J_2 - J_3 model.

B. Relevance for other systems

Here we considered a model with only localized spins. But we know from previous works on cuprates and heavy-fermions that charge fluctuations play a crucial role in destabilizing antiferromagnetic states.

In the context of cuprates, the AF Néel ordered phase of the insulating parent compounds corresponds to $\mathbf{Q}_{\text{AF}}^{\text{II}}$. The spin liquid phase introduced by Anderson *et al.*²⁴⁻²⁸ corresponds to the homogeneous spin liquid phase with Φ_2 non zero. The relation between the spin-liquid field and the superconducting order parameter has been discussed by Wen, Lee *et al.* in terms of gauge transformations.^{52,53} These gauge transformations are based on particle-hole transformations on the fermionic operators $\chi_{\mathbf{R}\sigma}$ that preserve the physical starting Heisenberg spin Hamiltonian but transform the spin-liquid fields into superconducting pairing terms.

Doping may be introduced more generally on the full J_1 - J_2 - J_3 model. In heavy fermions, we know that the localized quasiparticle states are associated with the f -electrons. These localized degrees of freedom directly related to magnetism are usually distinguishable from the itinerant charge degrees of freedom. Indeed, in Ce and Yb compounds, delocalized modes emerge from light conduction electrons; in actinides they emerge from the duality of the $5f$ orbitals that have a partial Mott-delocalized sector. In cuprates, such a localized spin - delocalized charge scenario cannot be clearly done. Especially at low doping, the adaption of the present spin-fermion model for cuprates should include the physics of the Mott transition. Therefore, doping the J_1 - J_2 - J_3 model should be realized appropriately in various manners adapted to each experimental motivation: typically, within Kondo+Heisenberg, t - J , or multi-orbital Hubbard models.

Inspired by the previous works of Wen, Lee *et al.*, we expect that the resulting charge fluctuations would strengthen the spin fluctuations and weaken the magnetically ordered phases that are predicted from a classical Heisenberg J_1 - J_2 - J_3 model. In turn, the spin-liquid phases are expected to remain stable, associated to superconducting instabilities. Invoking this general scenario, we predict that the symmetries of the resulting superconducting order parameters will result

from the point group symmetries of the spin-liquids. This scenario may be tested first with the superconducting instability observed in URu_2Si_2 inside the HO phase. More generally, this scenario also generalizes to 3D systems the spin-fluctuation pairing mechanism that was proposed for cuprates. Here, the link between the BCT lattice structure and the superconducting order parameter is natural. This spin-liquid mechanism driven by frustration on the BCT lattice may also be tested for the heavy-fermion superconductors CeRu_2Si_2 and CePd_2Si_2 , but in these systems valence fluctuation effects need to be carefully included.

Appart from superconductivity, we may also question whereas there is a connexion between HO in URu_2Si_2 and the magnetic-field induced non-fermi liquid properties observed in YbRh_2Si_2 . Indeed, this very unconventional heavy-fermion compound has a magnetically ordered ground state at ambient pressure but the associated local moment is relatively small. This suggests that frustration on the BCT lattice may be analyzed together with Kondo screening in this system.

VI. CONCLUSION

To summarize, we studied the frustrated J_1 - J_2 - J_3 quantum Heisenberg Hamiltonian in the BCT lattice using mean field approximations. Introducing variational parameters α_i , each intersite interaction is decoupled in the Weiss and the spin liquid channels. Our first observation corresponds to the fact that variationally the interactions always prefer a pure channel. Indeed, any intermediate value of α_i corresponds to a higher free energy than the one obtained with decoupling parameters $\alpha_i = 0$ (pure Weiss) or $\pi/2$ (pure spin-liquid).

Studying the model at $J_3 = 0$ for all temperatures T and at $T = 0$ for all values of coupling J_i , we find that the most stable variational solution corresponds to the purely magnetically ordered ones. Nevertheless, we also analyze and characterize the purely SL solutions that are the second most stable ones. Three possible different magnetically ordered phases emerge at low T , characterized by the ordering wave-vectors $(1, 1, 1)$, $(1/2, 1/2, 0)$, and $(1/2, 0, 0)$ that respectively correspond to the three different regimes dominated by J_1 , J_2 , or J_3 . Similarly, three different SL phases are also identified, the one dominated by J_1 corresponding to a non-homogeneous MSL state with commensurate ordering wave-vectors $(1, 1, 1)$, that is expected to survive beyond the mean-field. We also remarked that other variational solutions, including MSL states with a different wavevector $(0, 0, 1)$ or $(1, 0, 0)$ and mixed states with α_i non extreme, are energetically above but not so far from the three pure SL ones that are analyzed here. Fluctuations might stabilize some of these solutions as well.

Whilst the purely magnetically ordered phases are the most stable at the mean-field level, we expect fluctuations to be strong in the vicinity of the degeneracy lines separating the different ordering wave-vectors. It is very interesting to notice that the analogous degeneracy lines obtained for the three different SL solutions do not coincide with the ones obtained for the magnetically ordered solutions. We thus conclude that fluctuations should open a large area of parameters where

magnetic orders are destroyed, favoring the stabilization of SL phases.

Surprisingly, when considering four different fits of experimental INS datas on URu₂Si₂, we find in each case that this compound is close to the degeneracy line separating the (1, 1, 1) and (1/2, 0, 0) antiferromagnetic orders. We also find that, when considering the SL solutions, each of these four fits locates URu₂Si₂ well inside the MSL phase. This result suggests that fluctuations and frustration between J_1 and J_3 coupling should play a crucial role in the HO-AF transition that is induced by pressure at low T in this compound. The possible formation of a spatially modulated highly entangled state analogous to the MSL, emerging from frustration and fluctuations, could provide a key ingredient in the realization of the Hidden order phase.

The scenario presented here is very general and could be adapted and applied to study doped correlated systems with BCT structure, including possibly unconventional superconductors. In these cases, the inclusion of charge fluctuations in the model are necessary and have to be done carefully since they might also play a crucial direct role for the superconducting instabilities. Finally, the variational method that we introduced here could also be used for other models where a two-body interaction term can be decoupled in two different mean-field channels.

ACKNOWLEDGMENTS

We acknowledge the financial support of Capes-Cofecub Ph 743-12. CT is *bolsista Capes*. This research was also supported in part by the Brazilian Ministry of Science, Technology and Innovation (MCTI) and the Conselho Nacional de Desenvolvimento Científico e Tecnológico (CNPq). Research carried out with the aid of the Computer System of High Performance of the International Institute of Physics-UFRN, Natal, Brazil. The authors are grateful to Frédéric Bourdarot for usefull discussions.

Appendix A: Brillouin zones for the dual (bond) lattice

The choice of the phase of the modulation + or - on a given bond $\mathbf{R}\mathbf{R}'$ in Eq. (22) is of course not unique. At this stage we could not go further by considering the system in its whole generality. Motivated by experimental applications to URu₂Si₂, we may thus assume that the order parameter $\Phi_{\mathbf{Q}}$ lowers the lattice translation symmetry from BCT to tetragonal. This translation symmetry breaking corresponds to a doubling of the lattice unit cell, and may as well be characterized by various point group symmetry breaking. Indeed, the spin-liquid field $\varphi_{\mathbf{R}\mathbf{R}'}$ is defined on the dual (bond) lattice. Each of these possible point group symmetry breaking results from a non isotropic distribution of the phase modulation + or - on the bonds neighboring a given lattice site. Different possible orders belong to the same tetragonal lattice group but break different point group symmetries. It is remarkable that a MSL order can equivalently be characterized

by a point group symmetry or by an ordering wave-vector \mathbf{Q} belonging to the reciprocal space of the dual lattice. On the other side, the AF order is characterized by a wave-vector \mathbf{Q}_{AF} that belongs to the first Brillouin zone of the BCT lattice of sites, $\mathbf{BZ}_{\text{site}}^{\text{BCT}}$. We will thus later consider three other Brillouin zones, denoted $\mathbf{BZ}_{\text{bond}}^1$, $\mathbf{BZ}_{\text{bond}}^2$, and $\mathbf{BZ}_{\text{bond}}^3$, that correspond to the first Brillouin zones of the bonds connected with the couplings J_1 , J_2 , and J_3 respectively (see figure 1). Note that $\mathbf{BZ}_{\text{bond}}^2$ and $\mathbf{BZ}_{\text{bond}}^3$ look like two-dimensional Brillouin zones since the couplings J_2 and J_3 are inplane. We remark here that the present formalism at this stage can be applied to study both two-dimensional magnetism in compounds like cuprates where $J_1 \approx 0$ and three-dimensional magnetism in compounds like URu₂Si₂ for which J_1 drives the AF order. Since the BCT lattice has four times more bonds of kind 1 than sites, it appears that $\mathbf{BZ}_{\text{site}}^{\text{BCT}}$ is four times smaller than $\mathbf{BZ}_{\text{bond}}^1$. As a result, different wave-vectors \mathbf{Q} in $\mathbf{BZ}_{\text{bond}}^1$ characterizing different MSL bond orders, can be equivalent with each other from the AF point of view. For example, the ordering wave-vector $\mathbf{Q}_{\text{AF}}^{\text{I}}$ can be equivalently chosen to be (1, 1, 1), (1, 0, 0) or (0, 0, 1) when characterizing AF ordered phase on the BCT lattice. But these three vectors characterize three different MSL ordered states. A detailed analysis is given in Ref.,²¹ comparing the free energy of these three possible MSL ordered states. It was found that, when the degeneracy was left, (1, 1, 1) characterized the MSL state with the lowest free energy. Therefore, we choose to consider in this article only the results obtained with the modulation wave-vector $\mathbf{Q} = (1, 1, 1)$. Finally, note that the prefactors $1/2\sqrt{N}$ and $1/\sqrt{2N}$ in the Fourier transform relations (18, 19,20) are related to the number of sites or bonds which are relevant for each field: the BCT lattice considered here has N sites, $4N$ bonds connected by J_1 , and $2N + 2N$ bonds connected by J_2 and J_3 .

Appendix B: Bond singlet probabilities

Keeping in mind that the fermionic operators $\chi_{\mathbf{R}\sigma}$ represent quantum spin 1/2, each interaction term on a bond $\mathbf{R}\mathbf{R}'$ in the J_1 - J_2 - J_3 Hamiltonian (1) can be identified to an antiferromagnetic Heisenberg interaction:

$$\sum_{\sigma\sigma'} \chi_{\mathbf{R}\sigma}^\dagger \chi_{\mathbf{R}\sigma'} \chi_{\mathbf{R}'\sigma'}^\dagger \chi_{\mathbf{R}'\sigma} = \frac{1}{2} + 2\vec{S}_{\mathbf{R}} \cdot \vec{S}_{\mathbf{R}'}, \quad (\text{B1})$$

where $\vec{S}_{\mathbf{R}}$ and $\vec{S}_{\mathbf{R}'}$ are quantum spin 1/2 on sites \mathbf{R} and \mathbf{R}' . Integrating formally the other sites degrees of freedom of the many-body state characterizing the lattice, each local bond $\mathbf{R}\mathbf{R}'$ can be characterized by a probability $p_{\mathbf{R}\mathbf{R}'}^{\text{singlet}}$ to be in a singlet state. Invoking standard quantum spin algebra, we find the very general identity:

$$p_{\mathbf{R}\mathbf{R}'}^{\text{singlet}} = \frac{1}{4} - \langle \vec{S}_{\mathbf{R}} \cdot \vec{S}_{\mathbf{R}'} \rangle. \quad (\text{B2})$$

Introducing the variational parameter α_i that is appropriate to the bond $\mathbf{R}\mathbf{R}'$ as defined by Eq. (2), and invoking the mean-

field approximation decoupling in Weiss and spin-liquid channels as defined by Eqs. (3) and (4), we find the average

$$\sum_{\sigma\sigma'} \langle \chi_{\mathbf{R}\sigma}^\dagger \chi_{\mathbf{R}\sigma'} \chi_{\mathbf{R}\sigma'}^\dagger \chi_{\mathbf{R}\sigma} \rangle = 2m_{\mathbf{R}}m_{\mathbf{R}'} \cos^2(\alpha_i) - |\varphi_{\mathbf{R}\mathbf{R}'}|^2 \sin^2(\alpha_i). \quad (\text{B3})$$

Finally, within the variational mean-field approximation, the probability that a bond $\mathbf{R}\mathbf{R}'$ forms a singlet state is given by:

$$p_{\mathbf{R}\mathbf{R}'}^{\text{singlet}} = \frac{1}{2} - m_{\mathbf{R}}m_{\mathbf{R}'} \cos^2(\alpha_i) + \frac{|\varphi_{\mathbf{R}\mathbf{R}'}|^2}{2} \sin^2(\alpha_i), \quad (\text{B4})$$

where the kind of bond $i = 1, 2$ or 3 is defined on figure 1.

Appendix C: Saddle point equations for $J_3 = 0$

Using expression (35) with $\alpha_3 = \Phi_3 = J_3 = 0$, the seven saddle point equations for the free energy functional $F(\alpha_1, \alpha_2, \lambda_0, \Phi_1, \Phi_{\mathbf{Q}}, \Phi_2, S_{\mathbf{QAF}})$ are obtained from the following partial derivative expressions:

$$\begin{aligned} \frac{\partial F}{\partial \alpha_1} &= 2J_1 \cos \alpha_1 \sin \alpha_1 \left\{ 16 \sum_{\mathbf{k}} \frac{f(\Omega_{\mathbf{k}}^+) - f(\Omega_{\mathbf{k}}^-)}{\Delta \Omega_{\mathbf{k}}} \right. \\ &\times \left[2J_1 \sin^2 \alpha_1 (|\Phi_1 \gamma_{1,\mathbf{k}}|^2 + |\Phi_{\mathbf{Q}} \gamma_{1,\mathbf{k}+\mathbf{Q}/2}|^2) - J_{\mathbf{QAF}} \gamma_{1,\mathbf{QAF}} |S_{\mathbf{QAF}}|^2 \right] \\ &\left. + |\Phi_1|^2 + |\Phi_{\mathbf{Q}}|^2 + 8\gamma_{1,\mathbf{QAF}} |S_{\mathbf{QAF}}|^2 \right\}, \quad (\text{C1}) \end{aligned}$$

$$\begin{aligned} \frac{\partial F}{\partial \alpha_2} &= 4J_2 \sin \alpha_2 \cos \alpha_2 \left\{ \sum_{\mathbf{k}} \left\{ [f(\Omega_{\mathbf{k}}^+) + f(\Omega_{\mathbf{k}}^-)] |\Phi_2| \gamma_{2,\mathbf{k}} \right. \right. \\ &\left. \left. - 2 \left[\frac{f(\Omega_{\mathbf{k}}^+) - f(\Omega_{\mathbf{k}}^-)}{\Delta \Omega_{\mathbf{k}}} \right] J_{\mathbf{QAF}} \gamma_{2,\mathbf{QAF}} |S_{\mathbf{QAF}}|^2 \right\} \right. \\ &\left. + |\Phi_2|^2 + \gamma_{2,\mathbf{QAF}} |S_{\mathbf{QAF}}|^2 \right\}, \quad (\text{C2}) \end{aligned}$$

$$\begin{aligned} \frac{\partial F}{\partial \Phi_2} &= 2J_2 \sin^2 \alpha_2 \\ &\times \left\{ \sum_{\mathbf{k}} [f(\Omega_{\mathbf{k}}^+) + f(\Omega_{\mathbf{k}}^-)] \gamma_{2,\mathbf{k}} + 2|\Phi_2| \right\}, \quad (\text{C3}) \end{aligned}$$

$$\begin{aligned} \frac{\partial F}{\partial \Phi_1} &= 2J_1 \sin^2 \alpha_1 |\Phi_1| \\ &\times \left\{ 16 \sum_{\mathbf{k}} \left[\frac{f(\Omega_{\mathbf{k}}^+) - f(\Omega_{\mathbf{k}}^-)}{\Delta \Omega_{\mathbf{k}}} \right] J_1 \sin^2 \alpha_1 \gamma_{1,\mathbf{k}}^2 + 1 \right\}, \quad (\text{C4}) \end{aligned}$$

$$\begin{aligned} \frac{\partial F}{\partial \Phi_{\mathbf{Q}}} &= 2J_1 \sin^2 \alpha_1 |\Phi_{\mathbf{Q}}| \\ &\times \left\{ 16 \sum_{\mathbf{k}} \left[\frac{f(\Omega_{\mathbf{k}}^+) - f(\Omega_{\mathbf{k}}^-)}{\Delta \Omega_{\mathbf{k}}} \right] J_1 \sin^2 \alpha_1 \gamma_{1,\mathbf{k}+\mathbf{Q}/2}^2 + 1 \right\}, \quad (\text{C5}) \end{aligned}$$

$$\begin{aligned} \frac{\partial F}{\partial S_{\mathbf{QAF}}} &= 2J_{\mathbf{QAF}} S_{\mathbf{QAF}} \\ &\times \left\{ \sum_{\mathbf{k}} \left[\frac{f(\Omega_{\mathbf{k}}^+) - f(\Omega_{\mathbf{k}}^-)}{\Delta \Omega_{\mathbf{k}}} \right] J_{\mathbf{QAF}} - 1 \right\}, \quad (\text{C6}) \end{aligned}$$

$$\frac{\partial F}{\partial \lambda_0} = \sum_{\mathbf{k}} [f(\Omega_{\mathbf{k}}^+) + f(\Omega_{\mathbf{k}}^-)] - 1. \quad (\text{C7})$$

where $f(\omega) \equiv \frac{1}{1+\exp \beta \omega}$ denotes the Fermi function, and $\Delta \Omega_{\mathbf{k}} \equiv \Omega_{\mathbf{k}}^+ - \Omega_{\mathbf{k}}^- = 2\sqrt{(J_{\mathbf{QAF}})^2 |S_{\mathbf{QAF}}|^2 + 16(J_1^{\text{SL}})^2 [(\gamma_{1,\mathbf{k}})^2 |\Phi_1|^2 + (\gamma_{\mathbf{Q},\mathbf{k}})^2 |\Phi_{\mathbf{Q}}|^2]}$. In the following it will be convenient to introduce the field-dependent sums:

$$A_{\lambda_0} \equiv \frac{1}{N} \sum_{\mathbf{k}} [f(\Omega_{\mathbf{k}}^+) + f(\Omega_{\mathbf{k}}^-)], \quad (\text{C8})$$

$$A_{\Phi_2} \equiv \frac{1}{N} \sum_{\mathbf{k}} [f(\Omega_{\mathbf{k}}^+) + f(\Omega_{\mathbf{k}}^-)] \gamma_{2,\mathbf{k}}, \quad (\text{C9})$$

$$A_{\Phi_1} \equiv \frac{1}{N} \sum_{\mathbf{k}} \frac{f(\Omega_{\mathbf{k}}^+) - f(\Omega_{\mathbf{k}}^-)}{\Delta \Omega_{\mathbf{k}}} \gamma_{1,\mathbf{k}}^2, \quad (\text{C10})$$

$$A_{\Phi_{\mathbf{Q}}} \equiv \frac{1}{N} \sum_{\mathbf{k}} \frac{f(\Omega_{\mathbf{k}}^+) - f(\Omega_{\mathbf{k}}^-)}{\Delta \Omega_{\mathbf{k}}} \gamma_{1,\mathbf{k}\mathbf{Q}}^2, \quad (\text{C11})$$

$$A_{S_{\mathbf{QAF}}} \equiv \frac{1}{N} \sum_{\mathbf{k}} \frac{f(\Omega_{\mathbf{k}}^+) - f(\Omega_{\mathbf{k}}^-)}{\Delta \Omega_{\mathbf{k}}}. \quad (\text{C12})$$

After some standard algebra, the seven saddle point equations for $F(\alpha_1, \alpha_2, \lambda_0, \Phi_1, \Phi_{\mathbf{Q}}, \Phi_2, S_{\mathbf{QAF}})$ are rewritten as :

$$J_1 \sin 2\alpha_1 (8\gamma_{1,\mathbf{QAF}} |S_{\mathbf{QAF}}|^2 + |\Phi_1|^2 + |\Phi_{\mathbf{Q}}|^2) = 0, \quad (\text{C13})$$

$$J_2 \sin 2\alpha_2 (|\Phi_2|^2 + \gamma_{2,\mathbf{QAF}} |S_{\mathbf{QAF}}|^2) = 0, \quad (\text{C14})$$

$$J_2 \sin \alpha_2 (A_{\Phi_2} + 2|\Phi_2|) = 0, \quad (\text{C15})$$

$$J_1 |\Phi_1| \sin \alpha_1 (16J_1 \sin^2 \alpha_1 A_{\Phi_1} + 1) = 0, \quad (\text{C16})$$

$$J_1 |\Phi_{\mathbf{Q}}| \sin \alpha_1 (16J_1 \sin^2 \alpha_1 A_{\Phi_{\mathbf{Q}}} + 1) = 0, \quad (\text{C17})$$

$$J_{\mathbf{QAF}} S_{\mathbf{QAF}} (A_{S_{\mathbf{QAF}}} J_{\mathbf{QAF}} - 1) = 0, \quad (\text{C18})$$

$$A_{\lambda_0} = 1. \quad (\text{C19})$$

These equations may have some trivial solutions that correspond to giving α_1 and/or α_2 the extreme values 0 and $\pi/2$. This leads to four various cases that are defined in table I. Hereafter, the system of saddle-point relations (C13, C14, C15, C16, C17, C18, C19) is rewritten accordingly to the simplifications provided by each case. In all cases, we still have to solve the saddle point equation for the Lagrange multiplier λ_0 :

$$A_{\lambda_0} = 1. \quad (\text{C20})$$

For the other fields we are thus left with:

1. Trivial solutions: Case A

Here we consider the trivial cases where both α_1 and α_2 take extreme values $\pi/2$ or 0. There are naturally four possibilities that are analyzed sub-case by sub-case hereafter. Most of the saddle point equations are trivially satisfied, and we analyze here the relevant relations that still remain.

$$a. \text{ Sub-case } (\alpha_1, \alpha_2) = (0, 0)$$

This situation corresponds to the classical magnetic mean-field approximation. In this case, only magnetic order is considered, with the two possible ordering wave-vectors $\mathbf{Q}_{\text{AF}}^{\text{I}}$ and $\mathbf{Q}_{\text{AF}}^{\text{II}}$. The saddle point equation for $S_{\mathbf{Q}_{\text{AF}}}$ and a given ordering wave-vector is:

$$J_{\mathbf{Q}_{\text{AF}}} S_{\mathbf{Q}_{\text{AF}}} \left(A_{S_{\mathbf{Q}_{\text{AF}}}} J_{\mathbf{Q}_{\text{AF}}} - 1 \right) = 0. \quad (\text{C21})$$

$$b. \text{ Sub-case } (\alpha_1, \alpha_2) = (\pi/2, 0)$$

Here, the interplane spin liquid fields compete or coexist with the magnetic order originating from the inplane Weiss field J_2^{Weiss} . The saddle point equations for Φ_1 , $\Phi_{\mathbf{Q}}$, and $S_{\mathbf{Q}_{\text{AF}}}$ are:

$$J_1 |\Phi_1| \left(16J_1 A_{\Phi_1} + 1 \right) = 0, \quad (\text{C22})$$

$$J_1 |\Phi_{\mathbf{Q}}| \left(16J_1 A_{\Phi_{\mathbf{Q}}} + 1 \right) = 0, \quad (\text{C23})$$

$$J_2 \gamma_{2, \mathbf{Q}_{\text{AF}}} S_{\mathbf{Q}_{\text{AF}}} \left(2J_2 \gamma_{2, \mathbf{Q}_{\text{AF}}} A_{S_{\mathbf{Q}_{\text{AF}}}} - 1 \right) = 0. \quad (\text{C24})$$

$$c. \text{ Sub-case } (\alpha_1, \alpha_2) = (0, \pi/2)$$

Here, the different layers in (a, b) directions are decoupled from each other in a pure Weiss field channel. Inside each layer, the mean-field decoupling is purely spin-liquid. The saddle point equations for Φ_2 and $S_{\mathbf{Q}_{\text{AF}}}$ are:

$$J_2 \left(A_{\Phi_2} + 2|\Phi_2| \right) = 0, \quad (\text{C25})$$

$$J_1 \gamma_{1, \mathbf{Q}_{\text{AF}}} S_{\mathbf{Q}_{\text{AF}}} \left(8J_1 \gamma_{1, \mathbf{Q}_{\text{AF}}} A_{S_{\mathbf{Q}_{\text{AF}}}} - 1 \right) = 0. \quad (\text{C26})$$

$$d. \text{ Sub-case } (\alpha_1, \alpha_2) = (\pi/2, \pi/2)$$

This corresponds to a pure spin liquid state with interplane fields Φ_1 , $\Phi_{\mathbf{Q}}$, and inplane field Φ_2 . The saddle point equations are:

$$J_2 \left(A_{\Phi_2} + 2|\Phi_2| \right) = 0, \quad (\text{C27})$$

$$J_1 |\Phi_1| \left(16J_1 A_{\Phi_1} + 1 \right) = 0, \quad (\text{C28})$$

$$J_1 |\Phi_{\mathbf{Q}}| \left(16J_1 A_{\Phi_{\mathbf{Q}}} + 1 \right) = 0. \quad (\text{C29})$$

2. Case B

Here we consider that α_1 is fixed to an extreme value (0 or $\pi/2$), and α_2 is a free parameter. Since extremal values of α_2 have been already considered in case A, we thus assume the strict inequality $0 < \alpha_2 < \pi/2$. Eq. (C14) can thus be simplified as:

$$|\Phi_2|^2 + \gamma_{2, \mathbf{Q}_{\text{AF}}} |S_{\mathbf{Q}_{\text{AF}}}|^2 = 0, \quad (\text{C30})$$

Putting aside the trivial solution with vanishing fields, this relation requires an ordering wave-vector such that $\gamma_{2, \mathbf{Q}_{\text{AF}}} < 0$. Invoking the definition Eq. (33), we check easily that $\gamma_{2, \mathbf{Q}_{\text{AF}}^{\text{II}}} = -2$ and $\gamma_{2, \mathbf{Q}_{\text{AF}}^{\text{I}}} = +2$. Therefore we consider only the ordering wave-vector $\mathbf{Q}_{\text{AF}}^{\text{II}} = (1/2, 1/2, 0)$ for this case. Eq. (C30) enforces linearity between the fields:

$$|\Phi_2| = |S_{\mathbf{Q}_{\text{AF}}}| \sqrt{2}. \quad (\text{C31})$$

This relation and Eq. (C20) have to be completed by the other relevant saddle point equations that are rewritten as follows:

$$J_2 \left(A_{\Phi_2} + 2|\Phi_2| \right) = 0, \quad (\text{C32})$$

$$J_2 S_{\mathbf{Q}_{\text{AF}}} \left[4J_2 \cos^2(\alpha_2) A_{S_{\mathbf{Q}_{\text{AF}}}} + 1 \right] = 0, \quad (\text{C33})$$

and also:

$$a. \text{ Sub-case } \alpha_1 = 0:$$

$$\Phi_1 = \Phi_{\mathbf{Q}} = 0. \quad (\text{C34})$$

$$b. \text{ Sub-case } \alpha_1 = \pi/2:$$

$$J_1 |\Phi_1| \left(16J_1 A_{\Phi_1} + 1 \right) = 0, \quad (\text{C35})$$

$$J_1 |\Phi_{\mathbf{Q}}| \left(16J_1 A_{\Phi_{\mathbf{Q}}} + 1 \right) = 0. \quad (\text{C36})$$

3. Case C

This case corresponds to $\sin(2\alpha_2) = 0$ and a strict inequality $0 < \alpha_1 < \pi/2$. Here we first consider Eq. (C13), that is rewritten as:

$$8\gamma_{1, \mathbf{Q}_{\text{AF}}} |S_{\mathbf{Q}_{\text{AF}}}|^2 + |\Phi_1|^2 + |\Phi_{\mathbf{Q}}|^2 = 0. \quad (\text{C37})$$

Excluding the trivial solution with all fields vanishing, the AF ordering wave-vector must satisfy $\gamma_{1, \mathbf{Q}_{\text{AF}}} < 0$. Invoking the definition Eq. (31), we check easily that $\gamma_{1, \mathbf{Q}_{\text{AF}}^{\text{I}}} = -1$

and $\gamma_{1, \mathbf{Q}_{\text{AF}}^{\text{II}}} = +1/2$. Therefore we consider only the ordering wave vector $\mathbf{Q}_{\text{AF}}^{\text{I}} = (1, 1, 1)$ for this case, and Eq. (C37) reads:

$$8|S_{\mathbf{Q}_{\text{AF}}}|^2 = |\Phi_1|^2 + |\Phi_{\mathbf{Q}}|^2. \quad (\text{C38})$$

In case C, this relation, together with Eq. (C20) has to be completed by the following relevant saddle point equations:

$$J_1 |\Phi_1| \left(16J_1 A_{\Phi_1} \sin^2 \alpha_1 + 1 \right) = 0, \quad (\text{C39})$$

$$J_1 |\Phi_{\mathbf{Q}}| \left(16J_1 A_{\Phi_{\mathbf{Q}}} \sin^2 \alpha_1 + 1 \right) = 0. \quad (\text{C40})$$

and also:

a. Sub-case $\alpha_2 = 0$:

$$S_{\mathbf{Q}_{\text{AF}}} \left[A_{S_{\mathbf{Q}_{\text{AF}}}} (8J_1 \cos^2 \alpha_1 - 4J_2) + 1 \right] = 0, \quad (\text{C41})$$

$$\Phi_2 = 0. \quad (\text{C42})$$

b. Sub-case $\alpha_2 = \pi/2$:

$$J_2 \left(A_{\Phi_2} + 2|\Phi_2| \right) = 0, \quad (\text{C43})$$

$$S_{\mathbf{Q}_{\text{AF}}} \left(8J_1 A_{S_{\mathbf{Q}_{\text{AF}}}} \cos^2 \alpha_1 + 1 \right) = 0. \quad (\text{C44})$$

4. Case D

This case is in principle the most general one, where both α_1 and α_2 are considered as free parameters. Since extreme values 0 or $\pi/2$ have already been considered in previous cases, we assume here strict equalities $0 < \alpha_1 < \pi/2$ and $0 < \alpha_2 < \pi/2$. Therefore, Eqs. (C13) and (C14) can be simplified as:

$$8\gamma_{1, \mathbf{Q}_{\text{AF}}} |S_{\mathbf{Q}_{\text{AF}}}|^2 + |\Phi_1|^2 + |\Phi_{\mathbf{Q}}|^2 = 0, \quad (\text{C45})$$

$$|\Phi_2|^2 + \gamma_{2, \mathbf{Q}_{\text{AF}}} |S_{\mathbf{Q}_{\text{AF}}}|^2 = 0. \quad (\text{C46})$$

The only way to obtain a solution without all fields vanishing would require at least $S_{\mathbf{Q}_{\text{AF}}} \neq 0$. The corresponding AF ordering wave-vector \mathbf{Q}_{AF} would have to satisfy both $\gamma_{1, \mathbf{Q}_{\text{AF}}} < 0$ and $\gamma_{2, \mathbf{Q}_{\text{AF}}} < 0$. Nevertheless, invoking definitions (31) and (33), we check easily that $\gamma_{1, \mathbf{Q}_{\text{AF}}^{\text{I}}} < 0$ but $\gamma_{2, \mathbf{Q}_{\text{AF}}^{\text{I}}} > 0$, and $\gamma_{1, \mathbf{Q}_{\text{AF}}^{\text{II}}} > 0$ but $\gamma_{2, \mathbf{Q}_{\text{AF}}^{\text{II}}} < 0$. We thus conclude that neither $\mathbf{Q}_{\text{AF}}^{\text{I}}$ nor $\mathbf{Q}_{\text{AF}}^{\text{II}}$ ordering wave-vectors can lead to such a solution.

¹ C. Kittel, *Introduction to Solid State Physics - eighth edition* (John Wiley & Sons, 2005).
² G. Stewart, *Review of Modern Physics* **56**, 755 (1984).
³ P. Fulde, P. Thalmeier, and G. Zwicknagl, *Solid State Physics: Advances In Research and Applications* **60**, 1 (2006).
⁴ T. Palstra, A. Menovsky, J. Vandenberg, A. Dirkmaat, P. Kes, G. Nieuwenhuys, and J. Mydosh, *Physical Review Letters* **55**, 2727 (1985).
⁵ J. Mydosh and P. Oppeneer, *Review of Modern Physics* **83**, 1301 (2011).
⁶ J. Custers, P. Gegenwart, H. Wilhelm, K. Neumaier, Y. Tokiwa, O. Trovarelli, C. Geibel, F. Steglich, C. Pépin, and P. Coleman, *Nature* **424**, 524 (2003).
⁷ S. Friedemann, T. Westerkamp, M. Brando, N. Oeschler, S. Wirth, P. Gegenwart, C. Krellner, C. Geibel, and F. Steglich, *Nature Physics* **5**, 465 (2009).
⁸ J. Mignot, J. Flouquet, P. Haen, F. Lapiere, L. Puech, and J. Voiron, *Journal of Magnetism and Magnetic Materials* **76-7**, 97 (1988).
⁹ W. Knafo, S. Raymond, P. Lejay, and J. Flouquet, *Nature Physics* **5**, 753 (2009).
¹⁰ F. Steglich, J. Aarts, C. Bredl, W. Lieke, D. Meschede, W. Franz, and H. Schafer, *Physical Review Letters* **43**, 1892 (1979).

¹¹ N. Mathur, F. Grosche, S. Julian, I. Walker, D. Freye, R. Haselwimmer, and G. Lonzarich, *Nature* **394**, 39 (1998).
¹² A. Demuer, D. Jaccard, I. Sheikin, S. Raymond, B. Salce, J. Thomasson, D. Braithwaite, and J. Flouquet, *Journal of Physics - Condensed matter* **13**, 9335 (2001).
¹³ J. Bednorz and K. Muller, *Zeitschrift Fur Physik B-condensed Matter* **64**, 189 (1985).
¹⁴ H. Diep, *Physical Review B* **40**, 741 (1989).
¹⁵ H. Diep, *Physical Review B* **39**, 397 (1989).
¹⁶ E. Rastelli, S. Sedazzari, and A. Tassi, *Journal of Physics-condensed Matter* **1**, 4735 (1989).
¹⁷ R. Quartu and H. Diep, *Journal of Magnetism and Magnetic Materials* **182**, 38 (1998).
¹⁸ D. Loison, *Physica A* **275**, 207 (2000).
¹⁹ A. Sorokin and A. Syromyatnikov, *Journal of Experimental and Theoretical Physics* **113**, 673 (2011).
²⁰ C. Pépin, M. Norman, S. Burdin, and A. Ferraz, *Physical Review Letters* **106**, 106601 (2011).
²¹ C. Thomas, S. Burdin, C. Pépin, and A. Ferraz, *Physical Review B* **87**, 014422 (2013).
²² X. Montiel, S. Burdin, C. Pépin, and A. Ferraz, arXiv:1312.3653 (2013).
²³ A. Aharony and B. Huberman, *Journal of physics C - Solid state physics* **9**, L465 (1976).
²⁴ P. Fazekas and P. Anderson, *Philosophical magazine* **30**, 423 (1974).

- ²⁵ P. Anderson, G. Baskaran, Z. Zou, and T. Hsu, *Physical Review Letters* **58**, 2790 (1987).
- ²⁶ G. Baskaran, Z. Zou, and P. Anderson, *Solid state communications* **63**, 973 (1987).
- ²⁷ T. Rice, S. Gopalan, and M. Sigrist, *Europphys Letters* **23**, 445 (1993).
- ²⁸ X. Wen and P. Lee, *Physical Review Letters* **76**, 503 (1996).
- ²⁹ B. Canals and C. Lacroix, *Physical Review Letters* **80**, 2933 (1998).
- ³⁰ X. Wen, *Physical Review B* **65**, 165113 (2002).
- ³¹ L. Balents, *Nature* **464**, 199 (2010).
- ³² C. Lacroix, P. Mendels, and F. Mila, eds., *Introduction to Frustrated Magnetism*, Series in Solid-State Sciences, Vol. 164 (Springer, 2011) materials, Experiments, Theory.
- ³³ S. Yan, D. Huse, and S. White, *Science* **332**, 1173 (2011).
- ³⁴ Y. Iqbal, F. Becca, S. Sorella, and D. Poilblanc, *Physical Review B* **87**, 060405 (2013).
- ³⁵ H. Bethe, *Zeitschrift fur Physik* **71**, 205 (1931).
- ³⁶ U. Schollwock, *Review of Modern Physics* **77**, 259 (2005).
- ³⁷ C. Broholm, H. Lin, P. Matthews, T. Mason, W. Buyers, M. Collins, A. Menovsky, J. Mydosh, and J. Kjems, *Physical Review B* **43**, 12809 (1991).
- ³⁸ H. Kusunose, *Journal of the physical society of Japan* **81**, 023704 (2012).
- ³⁹ K. Sugiyama, H. Fuke, K. Kindo, K. Shimoata, A. Menovsky, J. Mydosh, and M. Date, *Journal of the Physical Society of Japan* **59**, 3331 (1990).
- ⁴⁰ F. Bourdarot, *Une autre vue sur URu₂Si₂* (Habilitation thesis, Grenoble, 2013).
- ⁴¹ J. Oitmaa and Z. Weihong, *Phys. Rev. B* **54**, 3022 (1996).
- ⁴² O. Sushkov, J. Oitmaa, and W. Zheng, *Physical Review B* **63**, 104420 (2001).
- ⁴³ A. Kalz, A. Honecker, S. Fuchs, and T. Pruschke, *Physical Review B* **83**, 174519 (2011).
- ⁴⁴ M. Maple, J. chen, Y. Dalichaouch, T. Kohara, C. Rossel, M. Torikachvili, M. McElfresh, and J. Thompson, *Physical Review Letters* **56**, 185 (1986).
- ⁴⁵ C. Broholm, J. Kjems, W. Buyers, P. Matthews, T. Palstra, A. Menovsky, and J. Mydosh, *Physical Review Letters* **58**, 1467 (1987).
- ⁴⁶ A. Villaume, F. Bourdarot, E. Hassinger, S. Raymond, V. Taufour, D. Aoki, and J. Flouquet, *Physical Review B* **78**, 012504 (2008).
- ⁴⁷ F. Bourdarot, E. Hassinger, S. Raymond, D. Aoki, V. Taufour, L. Regnault, and J. Flouquet, *Journal of the physical society of Japan* **79**, 064719 (2010).
- ⁴⁸ P. Riseborough, B. Coqblin, and S. Magalhaes, *Physical Review B* **85**, 165116 (2012).
- ⁴⁹ T. Das, *Physical Review B* **89**, 045135 (2014).
- ⁵⁰ P. Oppeneer, S. Elgazzar, J. Ruzs, Q. Feng, T. Durakiewicz, and J. Mydosh, *Physical Review B* **84**, 241102R (2011).
- ⁵¹ K. Kim, N. Harrison, M. Jaime, G. Boebinger, and J. Mydosh, *Physical Review Letters* **91**, 256401 (2003).
- ⁵² P. A. Lee, N. Nagaosa, and X. G. Wen, *Reviews of Modern Physics* **78**, 17 (2006).
- ⁵³ X.-G. Wen, *Quantum Field Theory of Many-Body Systems: From the Origin of Sound to an Origin of Light and Electrons*, Oxford Graduate Texts (Oxford University Press, 2004).